17. Lee YT, et al. (2011) Environmental and antigen receptor-derived signals support sustained surveillance of the lungs by pathogen-specific cytotoxic T lymphocytes. *J Virol* 85:4085–4094.
18. GeurtsvanKessel CH, et al. (2009) Dendritic cells are crucial for maintenance of tertiary lymphoid structures in the lung of influenza virus-infected mice. *J Exp Med* 206: 2339–2349.
19. Halle S, et al. (2009) Induced bronchus-associated lymphoid tissue serves as a general priming site for T cells and is maintained by dendritic cells. *J Exp Med* 206: 2593–2601.
20. Renegar KB, Small PA, Jr. (1991) Passive transfer of local immunity to influenza virus infection by IgA antibody. *J Immunol* 146:1972–1978.
21. Renegar KB, Small PA, Jr., Boykins LG, Wright PF (2004) Role of IgA versus IgG in the control of influenza viral infection in the murine respiratory tract. *J Immunol* 173: 1978–1986.
22. Mbawuike IN, et al. (1999) Mucosal immunity to influenza without IgA: an IgA knockout mouse model. *J Immunol* 162:2530–2537.
23. Harriman GR, et al. (1999) Targeted deletion of the IgA constant region in mice leads to IgA deficiency with alterations in expression of other Ig isotypes. *J Immunol* 162: 2521–2529.
24. Arulanandam BP, et al. (2001) IgA immunodeficiency leads to inadequate Th cell priming and increased susceptibility to influenza virus infection. *J Immunol* 166: 226–231.
25. Palladino G, Mozdzanowska K, Washko G, Gerhard W (1995) Virus-neutralizing antibodies of immunoglobulin G (IgG) but not of IgM or IgA isotypes can cure influenza virus pneumonia in SCID mice. *J Virol* 69:2075–2081.
26. Takahashi Y, et al. (2009) Protective immunity afforded by inactivated H5N1 (NIBRG-14) vaccine requires antibodies against both hemagglutinin and neuraminidase in mice. *J Infect Dis* 199:1629–1637.

nature COMMUNICATIONS

OPEN

ARTICLE

Received 14 Nov 2011 | Accepted 11 Jan 2012 | Published 14 Feb 2012

DOI: 10.1038/ncomms1677

Interferon-γ-producing immature myeloid cells confer protection against severe invasive group A *Streptococcus* infections

Takayuki Matsumura[1], Manabu Ato[1], Tadayoshi Ikebe[2], Makoto Ohnishi[2], Haruo Watanabe[2] & Kazuo Kobayashi[1]

Cytokine-activated neutrophils are known to be essential for protection against group A *Streptococcus* infections. However, during severe invasive group A *Streptococcus* infections that are accompanied by neutropenia, it remains unclear which factors are protective against such infections, and which cell population is the source of them. Here we show that mice infected with severe invasive group A *Streptococcus* isolates, but not with non-invasive group A *Streptococcus* isolates, exhibit high concentrations of plasma interferon-γ during the early stage of infection. Interferon-γ is necessary to protect mice, and is produced by a novel population of granulocyte–macrophage colony-stimulating factor-dependent immature myeloid cells with ring-shaped nuclei. These interferon-γ-producing immature myeloid cells express monocyte and granulocyte markers, and also produce nitric oxide. The adoptive transfer of interferon-γ-producing immature myeloid cells ameliorates infection in wild-type and interferon-γ-deficient mice. Our results indicate that interferon-γ-producing immature myeloid cells have a protective role during the early stage of severe invasive group A *Streptococcus* infections.

[1] Department of Immunology, National Institute of Infectious Diseases, 1-23-1 Toyama, Shinjuku-ku, Tokyo 162-8640, Japan. [2] Department of Bacteriology I, National Institute of Infectious Diseases, 1-23-1 Toyama, Shinjuku-ku, Tokyo 162-8640, Japan. Correspondence and requests for materials should be addressed to M.A. (email: ato@nih.go.jp).

Streptococcus pyogenes (group A *Streptococcus*; GAS) is one of the most common human pathogens. It causes a wide variety of infections, ranging from uncomplicated pharyngitis and skin infections to severe and even life-threatening manifestations such as streptococcal toxic shock syndrome (STSS) and necrotizing fasciitis. The mortality rates for STSS and necrotizing fasciitis are high (30–70%), even following prompt antibiotic therapy and debridement[1–4].

It is widely believed that myeloid cells including polymorphonuclear leukocytes (PMNs) have a central role in survival from GAS infections, and interferon (IFN)-γ is essential to full activation and proper function of PMNs. Notably, IFN-γ at the infection site is thought to be critical for protection; however, its increased systemic levels seem to be detrimental to survival after GAS infections[5]. Therefore, the appropriate regulation of cytokine-producing cells may be critical for survival and host defense against severe invasive GAS infections.

Myeloid cells with ring-shaped nuclei (ring cells) are present in the peripheral blood of patients with myeloproliferative diseases, but only rarely in healthy control subjects[6,7]. Ring cells are usually referred to as PMNs. However, not only Gr-1^{high} PMN-like ring cells, but also Gr-1^{low} mononuclear cell-like ring cells are present in the bone marrow, peripheral blood, and inflammatory infiltrates of mice[8]. Morphologically, a part of myeloid-derived suppressor cells (MDSCs) has ring-shaped nuclei[9,10]. MDSCs are potent suppressors of T-cell immunity, and their presence is associated with a poor clinical outcome in cancer. They are divided into 2 subtypes according to morphology and surface markers: Ly-6G$^-$ Ly-6C^{high} monocytic MDSCs and Ly-6G$^+$ Ly-6C^{low} granulocytic MDSCs[11,12]. Recent studies have demonstrated the considerable suppressive potential of MDSCs on T-cell immunity in autoimmune diseases, and also in chronic infections with intracellular pathogens, such as *Salmonella typhimurium*, *Candida albicans*, *Trypanosoma cruzi*, and *Toxoplasma gondii*[13]. However, the biological functions of ring cells in infectious diseases, and also the relationship between ring cells and MDSCs, remain largely unknown.

In the present study, IFN-γ-producing immature myeloid cells with ring-shaped nuclei (γIMCs), which originated from bone marrow precursor-like cells (BMPCs), are shown to be functionally and phenotypically distinct from MDSCs. We demonstrate that γIMCs have a protective role against severe invasive GAS infections, and possibly compensate for neutropenia.

Results

Role of IFN-γ in severe invasive GAS infections. To clarify the types of cytokines involved in severe invasive GAS infections, we first investigated the dynamics of cytokines in severe invasive and non-invasive GAS infections. As a model of disseminated infection in normally sterile sites, we intraperitonially (i.p.) infected GAS-susceptible C3H/HeN mice[14–17] with either severe invasive (*emm3* genotype *rgg* gene-mutated STSS strain, NIH34) or non-invasive (*emm3* genotype non-STSS (pharyngitis) strain, K33) GAS clinical isolates[18], and measured the levels of plasma cytokines. We detected no significant amount of plasma cytokines within 24 h of infection. By contrast, in mice infected with severe invasive GAS isolates, but not with non-invasive GAS isolates, we detected high levels of plasma IFN-γ; moreover, the levels increased rapidly at 48 h post-infection (Fig. 1a). Other cytokines, such as IL-1α, IL-1β, IL-4, IL-5, IL-12 p70 and IL-17, were scarcely detected in the plasma of mice infected with either severe invasive or non-invasive isolates. By contrast, in mice infected with severe invasive GAS isolates, the levels of IL-2, IL-10, and TNF increased transiently at 36 h post-infection.

Further, we evaluated whether IFN-γ is the host factor contributing to protection against severe invasive GAS infections, or to deterioration of STSS through an augmented inflammatory process. We i.p. administered mice with an anti-mouse IFN-γ neutralizing mAb (clone R4-6A2), on the day of infection with severe invasive GAS isolates. At 72 h post-infection, all of the mice administered with the IFN-γ neutralizing mAb died. By contrast, 50% of the mice treated with rat IgG as a control survived (Fig. 1b). These results are consistent with those of a previous study[5], in which mice treated with a different IFN-γ neutralizing mAb (clone XMG1.2) and IFN-γ knockout (*Ifng*$^{-/-}$) mice were more susceptible to lethal skin infection with the M-nontypeable GAS strain 64/14 than were control IgG-administered mice and wild-type mice, respectively. Thus, IFN-γ may act as a host defense factor against severe invasive GAS infections.

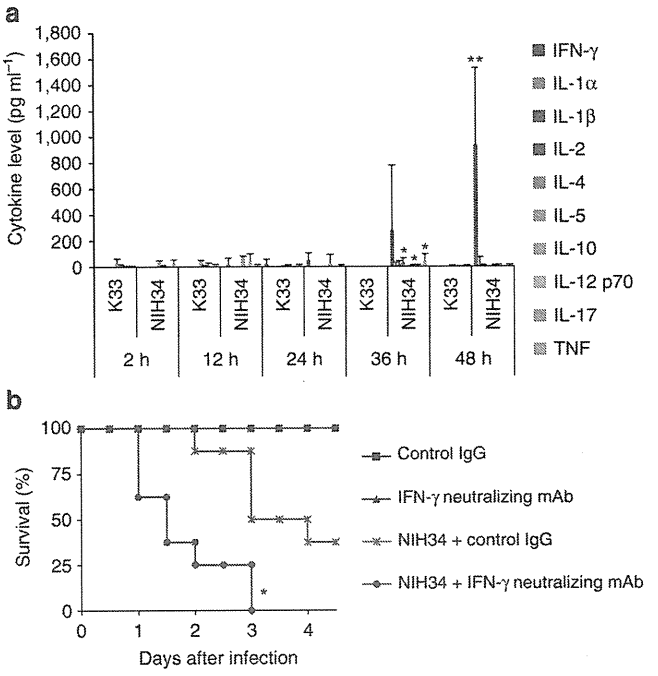

Figure 1 | IFN-γ is a host defense factor in mice infected with severe invasive GAS isolates. (**a**) C3H/HeN mice were i.p. inoculated with *S. pyogenes* (*emm3* genotype) clinical isolates (non-STSS, K33; STSS, NIH34; 3.0×10^7 CFU per mouse), and plasma cytokine levels were determined by FlowCytomix. Data are expressed as mean±s.d. for at least 2 independent experiments, using a total of 6-10 mice for each group. The differences compared with K33-infected mice were statistically significant ($^*P<0.05$, $^{**}P<0.01$) as determined by Student's *t*-test. (**b**) C3H/HeN mice were i.p. inoculated with NIH34 (3.0×10^7 CFU per mouse) in the presence of an IFN-γ neutralizing mAb (clone R4-6A2) (1 mg per mouse) or control rat IgG (1 mg per mouse). Survival was observed for 4 days post-infection. Mortality differences compared with infected mice in the presence of control IgG were statistically significant ($^*P<0.05$), as determined by a log-rank test. Survival curves were generated from two independent experiments, using a total of eight mice for each group.

A source of IFN-γ in severe invasive GAS infections. It is widely believed that T cells are a main source of IFN-γ in severe invasive GAS infections[19–21]. To identify the IFN-γ-producing cell types in mice infected with severe invasive GAS isolates, we used an *in vivo* intracellular cytokine synthesis (ICS) assay[22,23] to assess splenic IFN-γ production at 48 h post-infection. Unexpectedly, we revealed that Gr-1$^+$ CD11b$^+$ cells (but not TCR-β$^+$ TCR-γ/δ$^+$, CD4$^+$, or CD8$^+$ T cells, DX5$^+$ NK/NKT cells, or CD11c$^+$ MHC-II$^+$ dendritic cells) were a source of splenic IFN-γ in superantigen-insensitive C57BL/6 mice[24,25], and also in C3H/HeN mice (Fig. 2a and b). These Gr-1$^+$ cells appeared in the spleen on day 1 post-infection, subsequently increased in number, and were the major source of IFN-γ

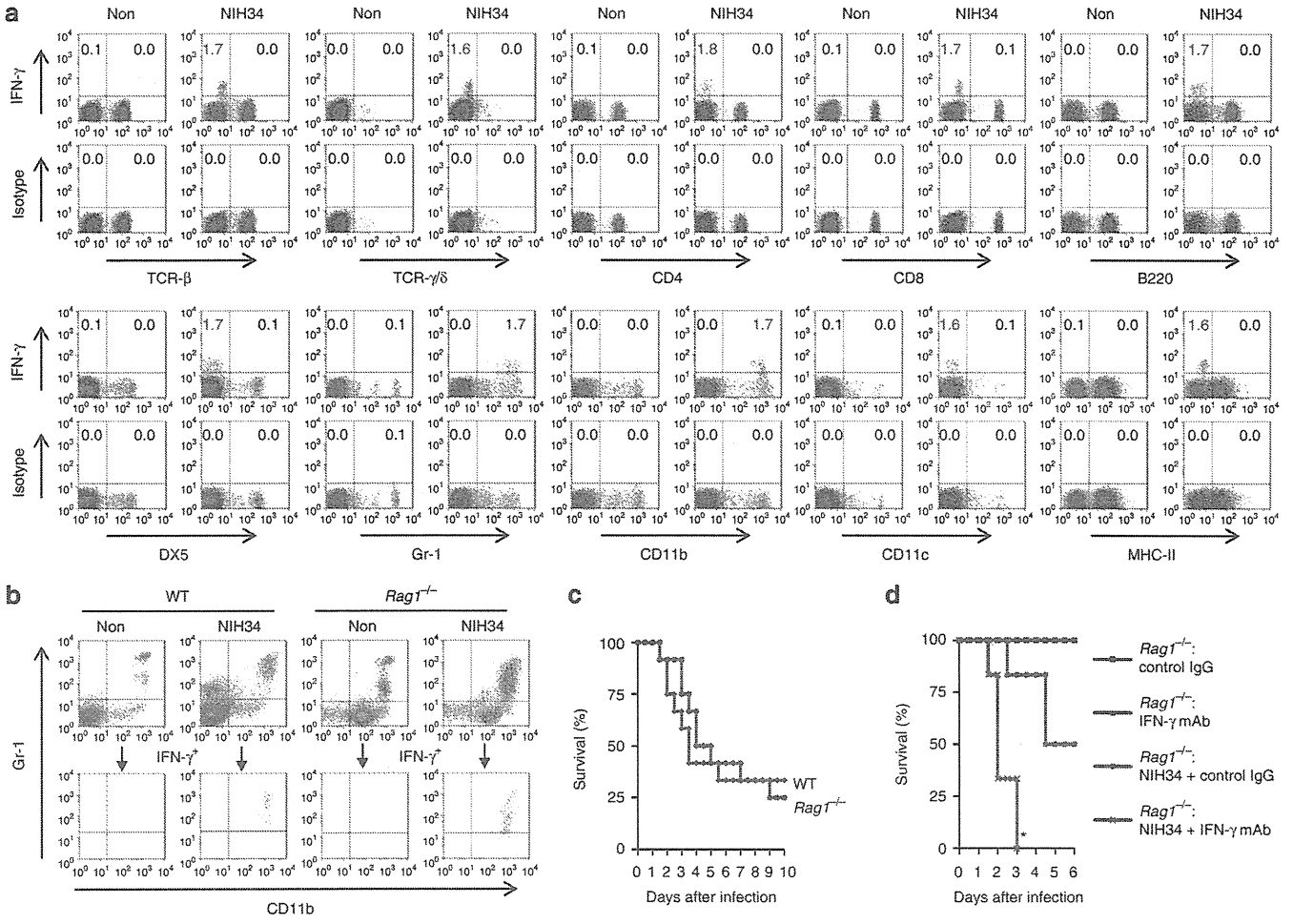

Figure 2 | CD11b$^+$ Gr-1$^+$ cells are the source of IFN-γ in severe invasive GAS infections. (**a**,**b**) C3H/HeN mice (**a**), C57BL per six mice (WT) (**b**), and *Rag1*$^{-/-}$ mice (**b**) with or without i.p. infection of NIH34 (3.0×10^7 CFU per mouse) for 42 h were i.v. injected with monensin. Six hours later, the mice were sacrificed and their splenocytes were immediately stained for the indicated markers, and analysed by ICS assay. (**a**) The numbers (%) in the plots represent the proportion of IFN-γ$^+$ subsets to total splenocytes. (**b**) Lower panels show the cells gated on the IFN-γ$^+$ population. Data are representative of three independent experiments. (**c**,**d**) WT and *Rag1*$^{-/-}$ mice were i.p. inoculated with NIH34 (3.0×10^7 CFU per mouse) in the absence (**c**) or presence (**d**) of an IFN-γ neutralizing mAb (clone R4-6A2) or control rat IgG (1 mg per mouse) as in Fig. 1b. Survival (in days) was observed as indicated. Survival curves were generated from 2 independent experiments, using a total of 12 mice for each group. (**d**) Mortality differences compared with infected mice in the presence of control IgG were statistically significant ($^*P<0.05$) as determined by a log-rank test.

throughout infection (Supplementary Fig. S1). By contrast, TCR-β$^+$ T cells and DX5$^+$ or NK1.1$^+$ NK cells, which are regarded as the sources of IFN-γ in GAS infections[15–17], produced small amounts of IFN-γ during the late stage (days 3–5 post-infection) of severe invasive GAS infections in C3H/HeN mice, but not in C57BL/6 mice. Notably, the accumulation of Gr-1$^+$ cells led to the clearance of infection from the spleen. Additionally, the administration of monensin, which blocks intracellular cytokine transport, did not induce spontaneous splenic production of IFN-γ (Fig. 2a and b; Supplementary Fig. S1).

To exclude the involvement of T cells in protection against severe invasive GAS infections, we investigated IFN-γ production in C57BL/6.RAG1 knockout (*Rag1*$^{-/-}$) mice, which have no mature B and T cells[26]. The ICS assay revealed that the cellular source of IFN-γ during severe invasive GAS infections was Gr-1$^+$ CD11b$^+$ cells in *Rag1*$^{-/-}$ mice, and also in C57BL/6 wild-type (WT) mice (Fig. 2b). We further examined the mortality of *Rag1*$^{-/-}$ mice during severe invasive GAS infections. We observed no significant difference in mortality between *Rag1*$^{-/-}$ and WT mice infected with severe invasive GAS isolates (Fig. 2c). Furthermore, similar to C3H/HeN mice (Fig. 1b), IFN-γ neutralizing mAb (clone R4-6A2)-treated *Rag1*$^{-/-}$ mice were more susceptible to severe invasive GAS infections than were control IgG-administered *Rag1*$^{-/-}$ mice (Fig. 2d). Our results indicate that mature B and T cells do not affect the mortality of infected mice, and that T cells have no protective effect during the early stage of severe invasive GAS infections.

Characterization of the early source of IFN-γ. Anti-Gr-1 mAb detects Ly-6C$^+$ monocytes and Ly-6G$^+$ PMNs. Therefore, to determine which subset of Gr-1$^+$ CD11b$^+$ cells is responsible for IFN-γ production during severe invasive GAS infections, we investigated the surface phenotype of IFN-γ-producing cells isolated from the spleens of mice at 48 h post-infection. The ICS assay revealed that IFN-γ-producing cells had the phenotype of monocytes (F4/80^{low} CX3CR1$^+$) and PMNs (Ly-6G$^+$ Ly-6C^{low}) (Fig. 3). Additionally, they expressed no lymphoid (CD27, IL-7Rα) or granulocyte-lineage (CCR3, Siglec-F, c-Kit, IL-5Rα (H7)) markers, but exhibited particular profiles of CCR2$^-$ CD31$^+$ CD34$^-$ CD38$^+$ CD44^{high} CD49d$^+$ CD62L$^+$ CD69$^+$ IL-5Rα (T21)^{high} Siglec-H$^-$ (Fig. 3; Supplementary Table S1). In this model, the most prominent GAS infection was present in the kidney[18,27]. In accordance with the bacterial burden in the peritoneal cavity, spleen and kidney, a higher proportion

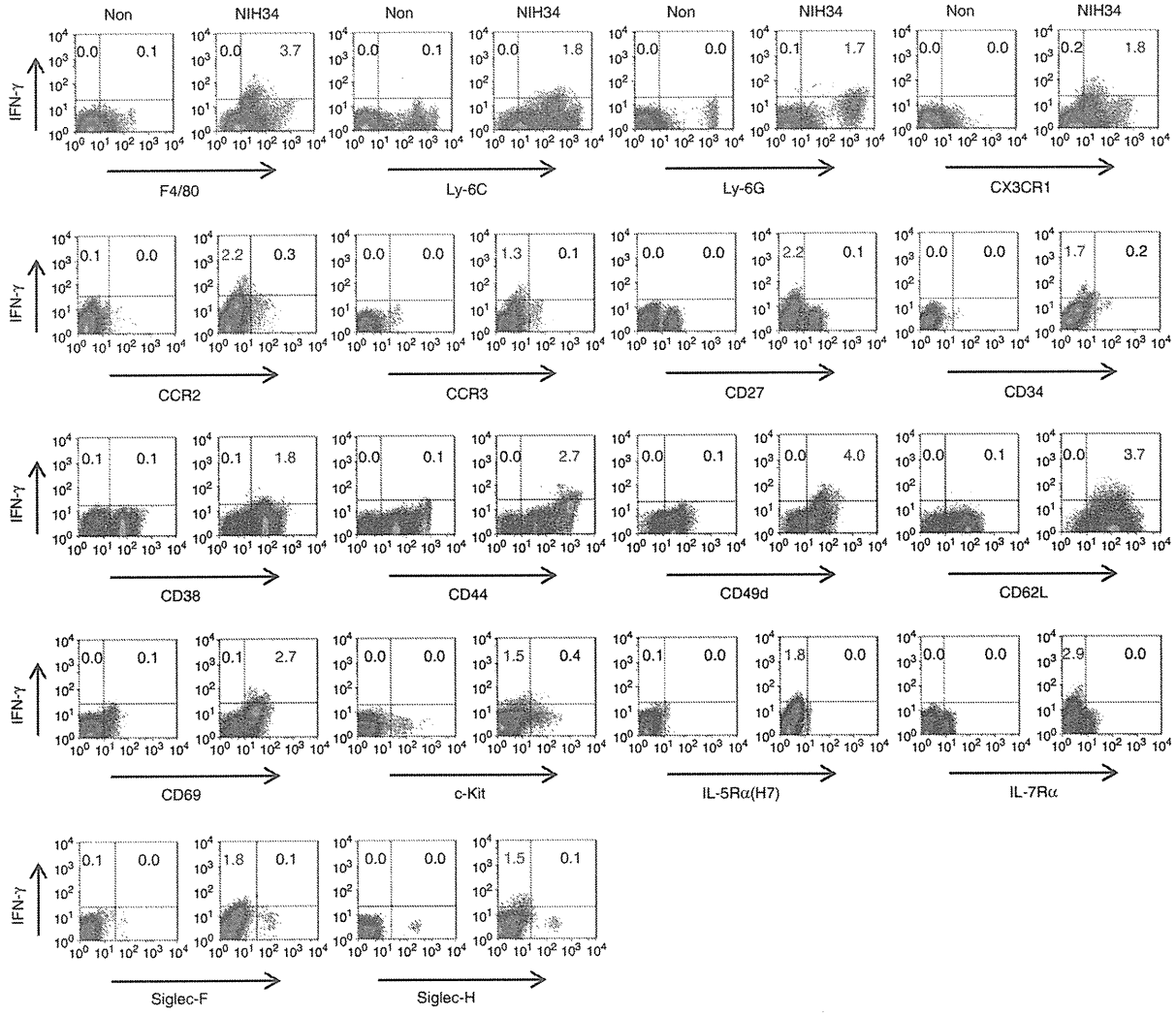

Figure 3 | IFN-γ-producing cells exhibit monocyte and PMN phenotypes in severe invasive GAS infections. C3H/HeN mice with or without i.p. infection of NIH34 (3.0×10^7 CFU per mouse) for 42 h were i.v. injected with monensin. Six hours later, the mice were killed and their splenocytes were immediately stained for the indicated markers, and analysed by the ICS assay. The numbers (%) in the plots represent the proportion of IFN-γ$^+$ subsets to total splenocytes. These data are representative of three independent experiments.

of IFN-γ-producing cells accumulated in the kidney of C3H/HeN mice, and also C57BL/6 mice i.p. infected with NIH34 (Supplementary Fig. S2). By contrast, lower proportion of IFN-γ-producing cells existed at the sites of infection. A skin-infection model yielded similar results (Supplementary Fig. S2). Furthermore, IFN-γ-producing cells were detected in the spleens from mice infected with various STSS strains[18,27] (Supplementary Fig. S3). These cells were also detected in the peripheral blood and (in particularly high frequency) the bone marrow from NIH34-infected mice (Fig. 4a–d; Supplementary Fig. S4). Interestingly, Siglec-F$^+$ eosinophils (Eos) stained with IL-5Rα (H7) and IL-5Rα (T21), whereas IFN-γ-producing cells stained well with T21, but not with H7 (Fig. 4e), suggesting that IFN-γ-producing cells were phenotypically distinct from Eos. IFN-γ-producing cells were also phenotypically distinct from Ly-6C^{low} CD31$^-$ PMNs (Fig. 4d). Moreover, the number and proportion of PMNs were markedly reduced in the spleen, peripheral blood, and bone marrow at 48 h post-infection (Fig. 4d and f), as reported in human STSS cases[28].

Immature myeloid cells as an early source of IFN-γ. The IFN-γ-producing cells expressed the phenotypic markers of monocytes/macrophages (F4/80 and CX3CR1) and PMNs (Ly-6G). Therefore, we sorted CD11b$^+$ CD11c$^-$ F4/80^{low} Ly-6G$^+$ cells from the spleens of infected mice and morphologically analysed them with May-Grünwald-Giemsa staining. The IFN-γ-producing CD11b$^+$ CD11c$^-$ F4/80^{low} Ly-6G$^+$ splenocytes were IMCs, but not monocytes/macrophages or PMNs. These IFN-γ-producing IMCs were large cells containing ring-shaped, non-segmented nuclei, with a coarse chromatin pattern[6–8] (Fig. 5a and b). The sorted cells were contaminated with a small number of PMNs; however, immunohistochemical analyses showed that IMCs, but not PMNs, were the source of IFN-γ (Fig. 5c). The cells with ring-shaped nuclei were also observed in the peritoneum, kidney, and spleen from i.p. infection model, and in the skin from subcutaneous (s.c.) infection model, whereas such cells were not observed in the spleen and kidney from non-infected or non-invasive K33 strain-infected mice (Fig. 5d and e). To determine whether IFN-γ-producing IMCs (γIMCs) are committed to the granulocyte or monocyte lineage, we cultured sorted CD11b$^+$ CD11c$^-$ F4/80^{low} Ly-6G$^+$ γIMCs *in vitro*, in the presence of G-CSF, M-CSF, GM-CSF or IL-5. We observed that G-CSF, M-CSF and IL-5 failed to promote differentiation and survival (Fig. 5f). By contrast, in the presence of GM-CSF, differentiated γIMCs increased their expression of CD11c, F4/80, DX5 and Siglec-F (Fig. 5g) with the polymorphonuclear phenotype (Fig. 5h). Such granulocyte-like cells showed

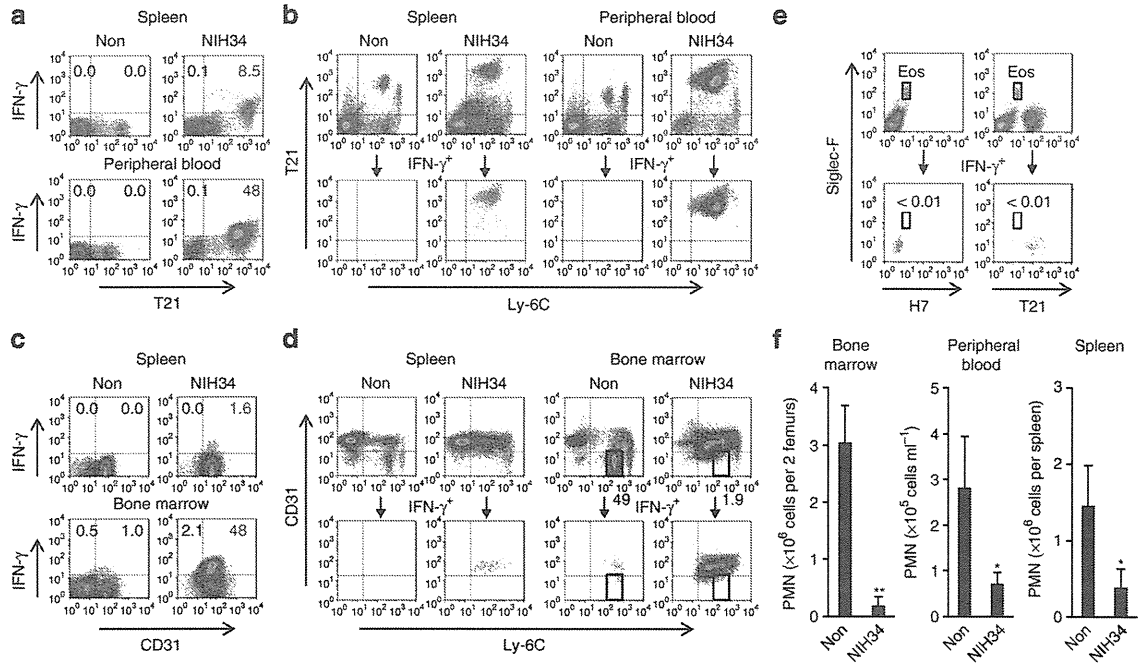

Figure 4 | IFN-γ-producing cells are detected in the peripheral blood and the bone marrow of GAS-infected mice. (**a**–**d**) Non-infected C3H/HeN mice or (**a**–**e**) mice i.p. infected with NIH34 (3.0×10^7 CFU per mouse) for 42 h were i.v. injected with monensin. Six hours later, the mice were killed and their splenocytes (**a**–**e**), peripheral blood cells (**a**,**b**), and bone marrow cells (**c**,**d**) were immediately stained for the indicated markers, and analysed by ICS assay. (**a**,**c**) The numbers (%) in the plots represent the proportion of IFN-γ$^+$ subsets to total cells. (**b**,**d**,**e**) Lower panels show the cells gated on the IFN-γ$^+$ population. (**d**,**e**) Rectangle gates in the plot represent mature granulocytes (**d**) and Eos (**e**). The numbers (%) in the plots represent the proportion of mature granulocytes (**d**) or IFN-γ$^+$ Eos (**e**) to total cells. Data are representative of three independent experiments. (**f**) The numbers of PMNs in the bone marrow, peripheral blood, and spleen from non-infected or NIH34-infected mice at 48 h. Data are expressed as mean ± s.d. ($n=3$). The differences compared with non-infected mice were statistically significant ($^*P<0.05$, $^{**}P<0.01$) as determined by Student's t-test.

reduced ability to produce IFN-γ (Fig. 5i), and were phenotypically different from c-Kit^{low} H7$^+$ Siglec-F$^+$ bone marrow-derived Eos and CCR3$^+$ H7$^+$ Siglec-F$^+$ splenic Eos[29]; (Supplementary Fig. S5). These results suggest that γIMCs are committed to the granulocyte lineage, but do not exist in the steady state, and produce IFN-γ during a specific stage of differentiation.

Nitric oxide (NO) is considered to be a main mechanism for controlling some infective agents. Myeloid cells are able to release NO in response to IFN-γ[30–33]; moreover, IFN-γ and NO-producing myeloid cells have been described in cancer[34]. Therefore, we investigated the ability of γIMCs to produce NO in response to GAS. When stimulated by autocrine and/or paracrine IFN-γ, γIMCs (but not than PMNs and granulocyte-like cells differentiated from γIMCs using GM-CSF) were able to produce NO, because their NO production was significantly blocked in the presence of IFN-γ neutralizing mAb (Fig. 5j).

Differentiation of precursor-like cells into γIMCs. Bone marrow contains the highest proportion of γIMCs (Fig. 4c and d). Therefore, we attempted to identify the precursors of γIMCs in the bone marrow of mice infected with severe invasive GAS isolates. Interestingly, analysis of the surface molecules revealed 2 distinct subsets of IFN-γ-producing cells (Fig. 6a): a minor and a major subset. The minor subset constituted 6.9 ± 3.2% of IFN-γ-producing bone marrow cells (Fig. 6b), and comprised CD11b$^+$ CD11c$^-$ F4/80^{low} Ly-6G$^+$ large cells (Supplementary Fig. S6), containing ring-shaped nuclei (BM-γIMCs) (Fig. 6c). On the basis of morphology and surface phenotype, these cells corresponded to splenic γIMCs (Sp-γIMCs) (Fig. 5a and b). Neither isolated BM-γIMCs nor Sp-γIMCs proliferated in the presence of GM-CSF (Figs 5f and 6d). These cells differed from metamyelocytes and immature neutrophils in non-infected bone marrow (Fig. 6c). The major subset of IFN-γ-producing cells comprised CD11b$^+$ CD11c^{low} F4/80$^+$ Ly-6G^{low} precursor-like cells (BMPCs) (Fig. 6b; Supplementary Fig. S6), which constituted 74.8 ± 13.7% of IFN-γ-producing cells (Fig. 6b). This subset consisted of ~10% monocyte-like ring cells and immature myeloid cells (Fig. 6c), which are phenotypically different from CD11b$^-$ Ly-6G$^-$ cells such as granulocyte–monocyte progenitors, common myeloid progenitors, and myelolymphoid progenitors[35]. In the presence of GM-CSF, isolated BMPCs proliferated (Fig. 6d) and differentiated into BM-γIMCs (Fig. 6c and e). Moreover, after 2 extra days of incubation with GM-CSF, differentiated BM-γIMCs increased their expression of CD11c, F4/80, DX5 and Siglec-F (Fig. 6f). The polymorphonuclear and cell surface phenotype (Supplementary Fig. S6) was similar to that of Sp-γIMCs cultured with GM-CSF (Fig. 5g and h). The differentiation of BMPCs into BM-γIMCs was totally blocked in the presence of IFN-γ neutralizing mAb; by contrast, this cytokine was dispensable for differentiation into granulocyte-like cells (Supplementary Fig. S6). These results are in accordance with the absence of Ly-6G$^+$ γIMCs in the spleen of GAS-infected C57BL6.*Ifng*$^{-/-}$ mice (Supplementary Fig. S7). The expression level of Ly-6G in PMNs was similar for WT and *Ifng*$^{-/-}$ mice (Supplementary Fig. S7). As with γIMCs and γIMC-differentiated granulocyte-like cells (Fig. 5i), the cells differentiated from BMPCs, after 2 extra days of incubation with GM-CSF, retained the ability to release IFN-γ in response to GAS; however, subsequent differentiation by GM-CSF reduced the ability to produce IFN-γ (Fig. 6g). A few IFN-γ-producing cells in non-infected mice were recognized in the same fraction as the BMPCs (Fig. 6a), and, therefore, it is possible that BMPCs exist in the naïve bone marrow. Our results suggest that IFN-γ-producing BMPCs are the precursors of γIMCs, and that their differentiation is dependent on autocrine and/or paracrine pathways involving

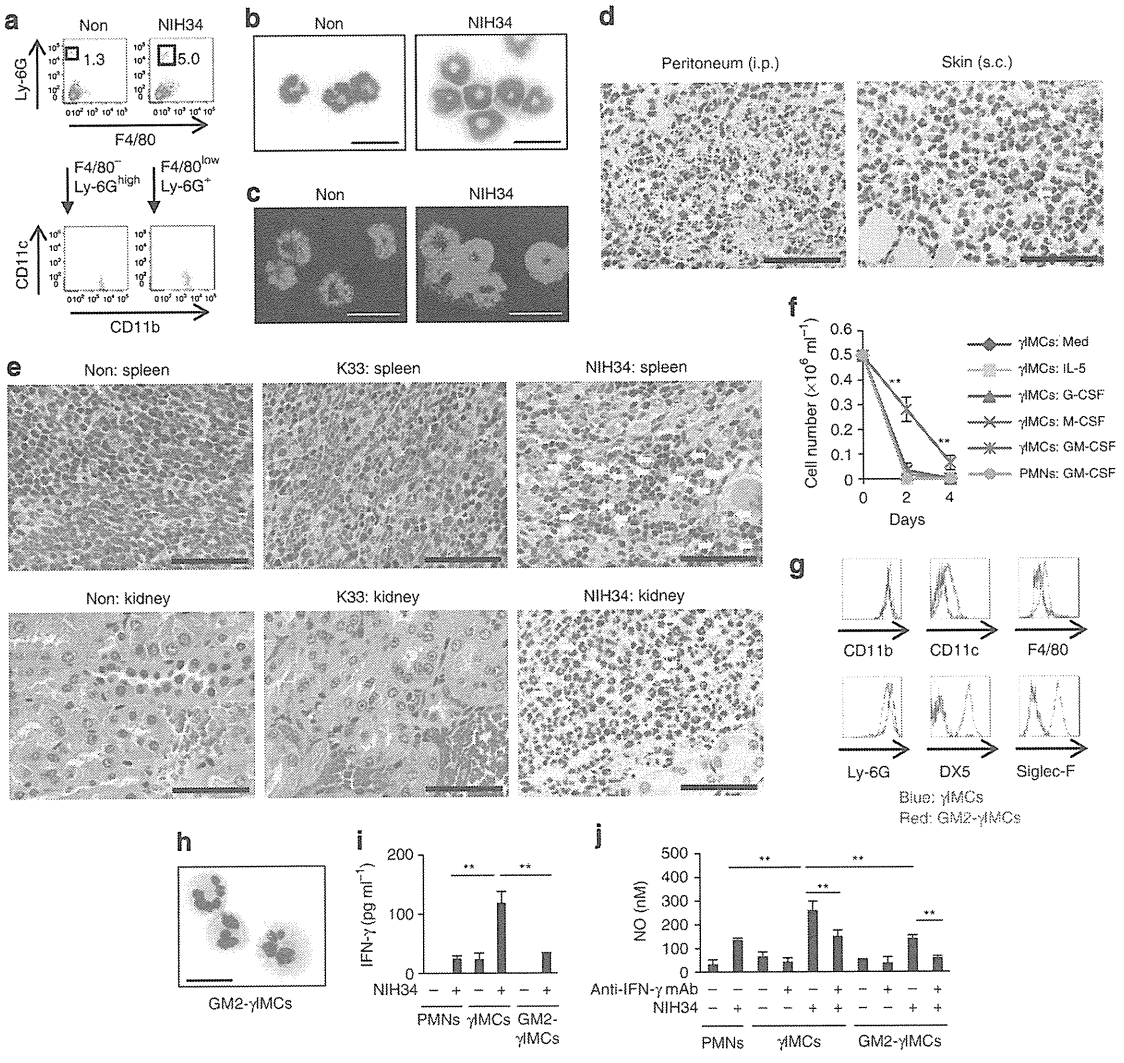

Figure 5 | γIMCs are the source of IFN-γ in severe invasive GAS infections. (**a**) CD11b$^+$ CD11c$^-$ F4/80$^-$ Ly-6G^{high} PMNs in splenocytes from non-infected C3H/HeN mice, or CD11b$^+$ CD11c$^-$ F4/80^{low} Ly-6G$^+$ γIMCs in splenocytes from mice infected with NIH34, were isolated by FACS. (**b**,**c**) Cytospin preparations of each sorted cell type were visualized with May-Grünwald-Giemsa staining (**b**), whereas intracellular IFN-γ (green, IFN-γ; red, nuclei) was visualized with a confocal laser microscopy (**c**). Scale bars, 20 μm. (**d**,**e**) Paraffin-embedded sections of peritoneum, from mice i.p. infected with NIH34 and skin from mice subcutaneously (s.c.) infected with NIH34 for 48 h (**d**), and of spleen and kidney from mice i.p. infected with or without K33 or NIH34 for 48 h, (**e**) were visualized with hematoxylin and eosin staining. The yellow arrows indicate the cells with ring-shaped nuclei. Scale bars, 100 μm. (**f**) Sorted IMCs were cultured with control medium (Med), G-CSF (50 ng ml^{-1}), M-CSF (10 ng ml^{-1}), GM-CSF (10 ng ml^{-1}), or IL-5 (10 ng ml^{-1}) for 2–4 days, and their absolute numbers were counted on the indicated days. Data are expressed as the average (mean±s.d.) of triplicate wells ($n=3$). The differences compared with Med were statistically significant (**$P<0.01$) as determined by Student's t-test. (**g**) γIMCs (blue line) and GM-CSF (2 days)-cultured γIMCs (GM2-γIMCs: red line) were stained for the indicated markers. Data are representative of three independent experiments. (**h**) Cytospin preparations of GM2-γIMCs were visualized with May-Grünwald-Giemsa staining. Scale bars, 20 μm. (**i**,**j**) γIMCs and GM2-γIMCs were cultured with erythromycin-treated NIH34 (MOI 100) in the presence of control rat IgG or an IFN-γ neutralizing mAb (clone R4-6A2) for 24 h. The levels of IFN-γ (**i**) and NO_2^- (**j**) in the culture supernatants were measured by ELISA and Griess reagent system, respectively. The average (mean±s.d.) of triplicate wells is shown. Statistical significance (**$P<0.01$) was determined by ANOVA.

IFN-γ. Notably, the BMPC-derived unclassified granulocyte-lineage, such as γIMCs (but not immature PMNs), seems to appear during severe invasive GAS infections.

Distinction between γIMCs and MDSCs. MDSCs are composed of F4/80$^-$ or F4/80^{low} granulocytic MDSCs with ring-shaped nuclei, and F4/80$^+$ monocytic MDSCs[10,11]. They can produce IFN-γ[13]. Furthermore, granulocytic/monocytic MDSCs differentiate into CD11c$^+$ F4/80$^+$ Gr-1$^+$ cells[12], as do γIMCs (Fig. 5g). To identify the relationship between the types of γIMCs observed during severe invasive GAS infections and MDSCs, we investigated the ability of γIMCs to suppress T-cell responses. As reported previously, *in vitro*-differentiated Ly-6C$^+$ Ly-6G^{low} F4/80$^+$ MDSCs[9] spontaneously produced IFN-γ (Fig. 7a), and inhibited Ag-specific T-cell proliferation and IFN-γ production from T cells (Fig. 7b). Conversely, purified γIMCs failed to inhibit T-cell responses (Fig. 7c), suggesting that γIMCs are functionally distinct from MDSCs. Additionally, MDSCs markedly decreased in number and lost the ability to produce IFN-γ when cultured *in vitro* with severe invasive GAS isolates (Fig. 7a). Furthermore, CCR2$^-$ CX3CR1$^+$ CD31$^+$ γIMCs are phenotypically different from CCR2$^+$ CX3CR1$^-$ CD31$^-$ granulocytic MDSCs and CCR2^{high} CX3CR1$^-$ CD31$^+$ monocytic MDSCs (Supplementary

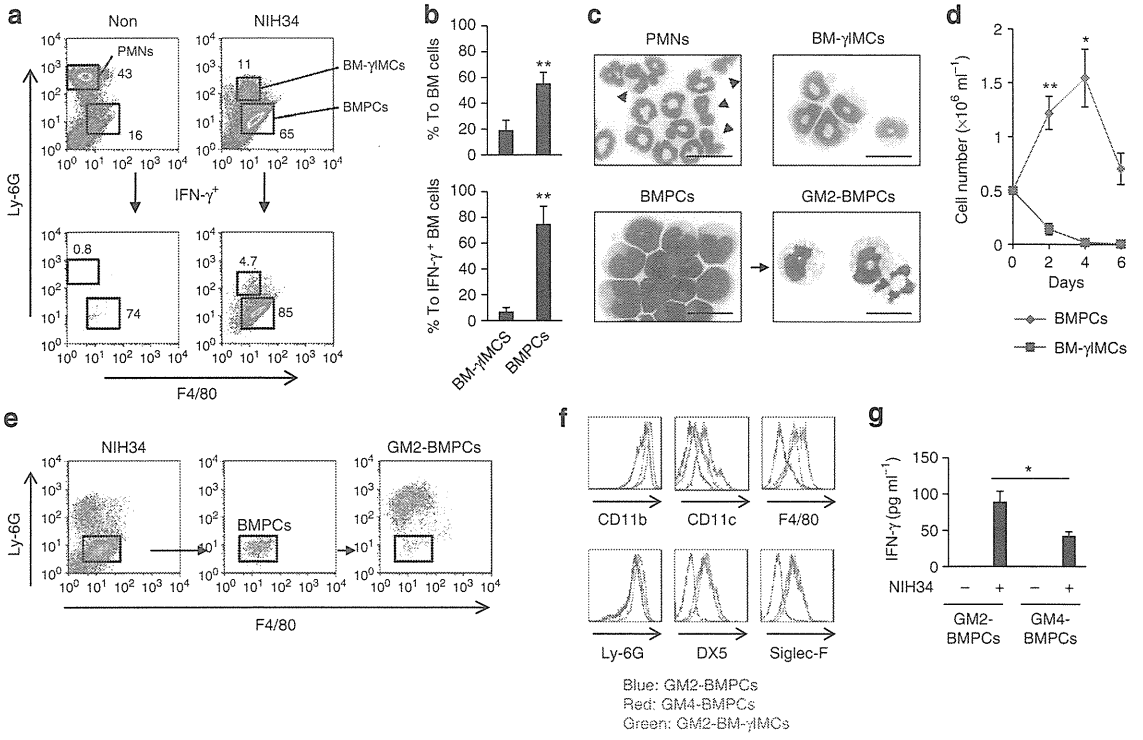

Figure 6 | BMPCs differentiate into γIMCs in the presence of GM-CSF. (**a**) C3H/HeN mice non-infected or i.p. infected with NIH34 (3.0×10^7 CFU per mouse) for 42 h were i.v. injected with monensin. Six hours later, the mice were killed and their bone marrow cells were immediately stained for the indicated markers, and analysed by ICS assay. Lower panels show the cells gated on the IFN-γ$^+$ population. The numbers (%) in the plots represent the proportion of PMNs, BM-γIMCs, and BMPCs to total (upper panels) and IFN-γ$^+$ (lower panels) bone marrow cells. (**b**) Proportion (%) of BM-γIMCs and BMPCs to bone marrow cells (upper panel) or IFN-γ-producing bone marrow cells (lower panel). Data are expressed as mean±s.d. ($n=3$). The differences compared with the proportion of BM-γIMCs were statistically significant ($^{**}P<0.01$) as determined by Student's *t*-test. (**c**) Cytospin preparations of sorted PMNs, BM-γIMCs, BMPCs, and GM-CSF (2 days)-cultured BMPCs (GM2-BMPCs) were visualized with May-Grünwald-Giemsa staining. Arrowheads indicate stab neutrophils or metamyelocytes. Scale bars, 20 μm. (**d**) Sorted BMPCs and BM-γIMCs were cultured with GM-CSF (10 ng ml^{-1}) for 2–6 days, and their absolute numbers were counted on the indicated days. Data are expressed as mean±s.d. ($n=3$). The differences in proliferation increase were statistically significant ($^*P<0.05$, $^{**}P<0.01$) as determined by Student's *t*-test. (**e**) Flow cytometry profile of infected bone marrow cells (left), sorted BMPCs (middle), and GM2-BMPCs (right). Rectangles show a sorting gate of BMPCs. (**f**) GM-CSF-cultured BMPCs (2 days or 4 days; GM2-BMPCs, blue line; GM4-BMPCs, red line) and BM-γIMCs (2 days; GM2-BM-γIMCs, green line) were stained for the indicated markers. Data are representative of 3 independent experiments. (**g**) IFN-γ production from BMPCs. GM2-BMPCs or GM4-BMPCs were cultured with erythromycin-treated NIH34 (MOI 100) in the presence of control rat IgG or an IFN-γ neutralizing mAb (clone R4-6A2) for 24 h. The level of IFN-γ in the culture supernatants was measured by ELISA. The average (mean±s.d.) of triplicate wells is shown. Statistical significance ($^*P<0.05$) was determined by Student's *t*-test.

Table S1). Taken together, our results indicate that γIMCs, which appear in association with severe invasive GAS infections, comprise a novel subset of IFN-γ-producing cells, but not MDSCs.

Role of γIMCs in severe invasive GAS infections. To elucidate the protective role of γIMCs, we employed an adoptive transfer system using WT or *Ifng*$^{-/-}$ mice. CD11b$^+$ CD11c$^-$ F4/80^{low} Ly-6G$^+$ γIMCs were purified from the spleens of WT mice infected with severe invasive GAS at day 2, and transferred into recipient mice. These mice were infected with a lethal dose of severe invasive GAS isolates (5×10^7 CFU (high dose)/WT mouse, 1×10^7 CFU (low dose)/*Ifng*$^{-/-}$ mouse), and the bacterial loads (CFUs) in the blood were quantified. At 24 h post-infection, γIMC-recipients and IFN-γ-treated mice had significantly lower bacterial loads in the blood than did control mice (Fig. 8a–c). Additionally, all control mice and all IFN-γ-treated mice died. By contrast, 100% of high dose-infected WT recipients and low dose-infected *Ifng*$^{-/-}$ recipients of γIMCs, and also low dose-infected WT mice, survived until 60 h post-infection (Fig. 8d–f). Our results indicate that IFN-γ successfully improved the bacterial clearance, but that systemic IFN-γ treatment was detrimental to survival following GAS infections (Fig. 8a,c,d and f). Thus, it appears that γIMCs have a protective role in severe invasive GAS infections.

Discussion

Previous studies have indicated that T cells and NK cells may have a role in the production of IFN-γ during GAS infections[5,15–17,19–21]. In the present study, we have demonstrated for the first time that γIMCs in the peritoneal cavity, skin, spleen, kidney, peripheral blood and bone marrow (but not T cells or NK cells) produce IFN-γ *in vivo* during the early stage of severe invasive GAS infections. The intensity of IFN-γ production is comparable among γIMCs, T cells, and NK cells, but production by γIMCs takes place sooner than that by T cells and NK cells. Moreover, throughout the course of GAS infection, γIMCs are the main IFN-γ-producing cells in the spleen. We further observed that IFN-γ neutralized *Rag*$^{-/-}$ mice succumbed to severe GAS infection at a similar rate to WT mice. Taken together, our results indicate that γIMCs comprise the major source of IFN-γ during the early stage of severe invasive GAS infections, and that they have an important protective role.

Notably, IFN-γ administration reduced the number of bacteria in the blood, whereas the transfer of γIMCs, but not of IFN-γ,

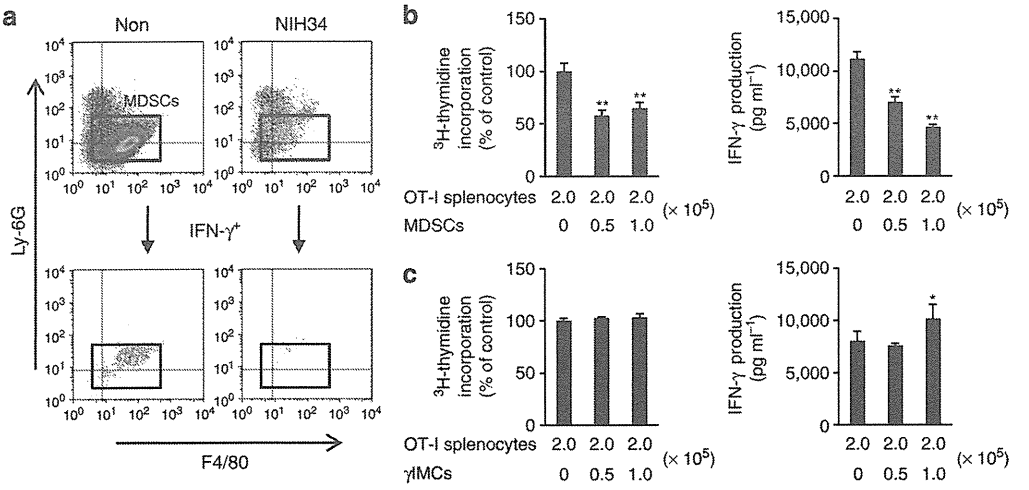

Figure 7 | γIMCs are functionally different from MDSCs. (**a**) C57BL/6 mouse bone marrow-derived MDSCs were differentiated *in vitro* with 40 ng ml^{-1} GM-CSF for 4 days. MDSCs were then incubated with or without severe invasive GAS isolates (NIH34; MOI 1) in the presence of brefeldin A (10 μg ml^{-1}). Three hours later, the cells were immediately stained for F4/80, Ly-6G, and IFN-γ, and analysed by ICS assay. Lower panels show the cells gated on the IFN-γ$^+$ population. (**b**,**c**) CD11b$^+$ CD11c$^-$ Ly-6C$^+$ Ly-6G^{low} *in vitro*-differentiated MDSCs, and CD11b$^+$ CD11c$^-$ F4/80^{low} Ly-6G$^+$ γIMCs, in the spleen from C57BL per six mice infected with NIH34 (3.0×10^7 CFU per mouse) for 48 h were isolated by FACS. Purified MDSCs (**b**) or purified γIMCs (**c**) were cultured at the indicated ratio with 2.0×10^5 splenocytes from C57BL/6.OT-I mice in the presence of antigenic $OVA_{357-364}$ peptides. Cell proliferation was measured using [^{3}H] thymidine uptake, and the level of IFN-γ in the culture supernatants was measured by ELISA. Each experiment was performed in triplicate. Mean±s.d. is shown. The differences compared with OT-I splenocytes alone were statistically significant (*$P<0.05$, **$P<0.01$) as determined by ANOVA. Data are representative of three independent experiments.

improved the survival rate of mice following GAS infection. Therefore, IFN-γ was necessary, but not sufficient, to protect mice from severe invasive GAS infections. We propose that NO production from γIMCs (which is restrictively controlled by IFN-γ), perhaps combined with that from other myeloid cells, may have a critical defensive role during the early stage of infection. In systemic GAS infection, γIMCs are deployed in various infected tissues; thus, the derived IFN-γ, NO, and/or as yet unidentified protective factors may promote the development of innate immune responses for the activation of phagocytes. However, we were unable to exclude the possibility that excessive quantities of IFN-γ secreted by T cells following superantigens stimulation, by NK cells, and even by γIMCs at the late stage of infection, are detrimental to survival following GAS infections, by exacerbating inflammatory responses and organ injury.

γIMCs express phenotypic markers of the monocyte/macrophage and granulocyte lineages, and are phenotypically different from other Ly-6C$^+$ cells, such as inflammatory and resident monocytes[11,36]. Mature PMNs, immature PMNs, and their progenitors proliferate or maintain their survival in the presence of G-CSF[37]. By contrast, in the present study, γIMCs did not survive in the presence of G-CSF. However, in the presence of GM-CSF, they differentiated into a PMN-like phenotype. Thus, γIMCs are distinct from the PMN lineage that develops during steady-state haematopoiesis. In the presence of GM-CSF, γIMCs possessed the ability to express a specific marker for Eos, Siglec-F. Nevertheless, based on staining with H7 and T21, they were distinct from Siglec-F$^+$ splenic Eos. Our observation that γIMCs failed to proliferate in response to IL-5 are consistent with the previous finding that T21 mAb may recognize IL-5Rα and other myeloid cell surface protein(s)[38]. Thus, γIMCs are unlikely to be committed to an Eos lineage; similarly, they are phenotypically different from DX5$^+$ basophils and basophil lineage-committed progenitors[39].

Granulocytic MDSCs are very similar to γIMCs in terms of surface markers (CD11b, F4/80, Ly-6C, Ly-6G, CD44, CD49d, and CD62L)[10,11], dependency on a growth factor (GM-CSF)[12], and cytokine production profile (IFN-γ)[13]. However, in the present study, we reveal that MDSCs did not produce IFN-γ in response to *in vitro* GAS infections. This is consistent with the previous finding that MDSCs from septic mice did not produce IFN-γ[40]. MDSCs are believed to originate from, or be accelerated by, the blockade of normal haematopoiesis during chronic inflammation or in a tumour-bearing state. γIMCs and MDSCs may therefore be closely related cell populations, and their differentiation and function may be regulated by the host circumstances.

On the basis of our present findings, we conclude that γIMCs are committed to an unclassified granulocyte lineage with an immature phenotype, and that such cells have the potential to replenish granulocyte populations. Moreover, GM-CSF is essential for the extraordinary state, such as severe systemic infection, but not for normal haematopoiesis[41]. The replacement of GM-CSF-dependent γIMCs may be regarded as a marked shift to the left of the leukocyte differential, with many immature granulocytes in automated cell counting. This is a characteristic of severe invasive GAS infections in our mouse model and also in human diseases[4,28]. The role of γIMCs in other infections and inflammatory diseases remains to be elucidated.

In the present study, we reveal that γIMCs differentiate from a subpopulation of CD11b$^+$ CD11c^{low} F4/80$^+$ Ly-6G^{low} cells in the bone marrow; this is known as a monocyte lineage. No γIMCs were detected in *Ifng*$^{-/-}$ mice infected with GAS, and IFN-γ-producing BMPCs (but not γIMCs) failed to differentiate into granulocyte-like cells in the presence of an IFN-γ neutralizing mAb. These observations suggest that the generation of γIMCs depends on the production of IFN-γ by BMPCs themselves. IFN-γ derived from BMPCs and γIMCs may be a key component of haematopoiesis during innate and adaptive immune responses, as shown in cases of malaria and *Mycobacterium avium* infection[35,42]. In the steady state, a few IFN-γ-producing cells existed in the Ly-6C^{low} CD31$^+$ fraction, including mixed progenitors of bone marrow[43]. Thus, we cannot exclude the possibility that BMPCs exist in non-infected bone marrow and have potential to produce IFN-γ, and that a subset of bone marrow cells can produce IFN-γ for the reproduction of haematopoietic stem cells[42].

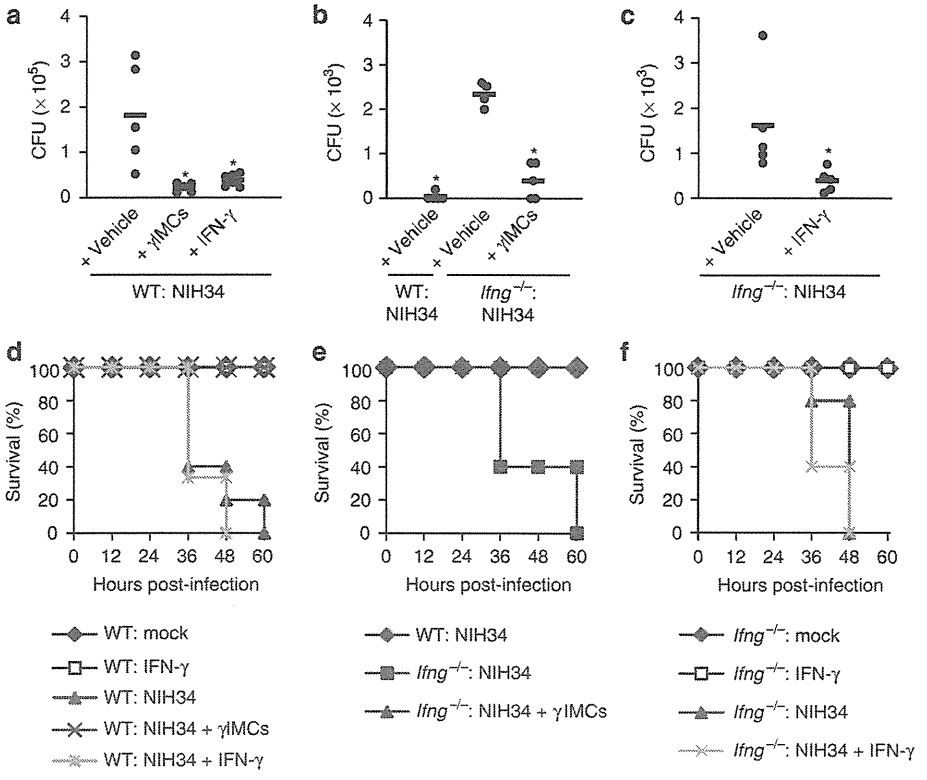

Figure 8 | γIMCs participate in protection against severe invasive GAS infections. (**a**–**f**) $CD11b^+$ $CD11c^-$ $F4/80^{low}$ $Ly\text{-}6G^+$ γIMCs in the spleen from C57BL/6 WT mice infected with NIH34 (3.0×10^7 CFU per mouse) for 48 h were isolated by FACS. WT or $Ifng^{-/-}$ mice i.v. received 3.0×10^6 γIMCs, or were i.p. treated with IFN-γ (10 ng per mouse). (**a**,**d**) WT mice ($n=5$), WT recipients of γIMCs ($n=5$), and mice i.p. treated with IFN-γ ($n=6$) were i.p. inoculated with NIH34 (5.0×10^7 CFU per mouse). (**b**,**e**) WT mice ($n=5$), $Ifng^{-/-}$ mice ($n=5$), and $Ifng^{-/-}$ recipients of γIMCs ($n=5$) were i.p. inoculated with NIH34 (1.0×10^7 CFU per mouse). (**c**,**f**) $Ifng^{-/-}$ mice ($n=5$) and $Ifng^{-/-}$ mice i.p. treated with IFN-γ ($n=5$) were i.p. inoculated with NIH34 (1.0×10^7 CFU per mouse). (**a**,**b**,**c**) The CFU of NIH34 in the peripheral blood was determined at 24 h post-infection. The differences compared with NIH34-infected WT mice (**a**) or NIH34-infected $Ifng^{-/-}$ mice (**b**,**c**) were statistically significant ($^*P<0.05$) as determined by the Mann–Whitney *U*-test. (**d**,**e**,**f**) Survival was observed for 60 h post-infection. Data are representative of two independent experiments.

Ring cells are present in the blood and bone marrow of humans, especially patients with chronic myeloproliferative diseases[6–8] but only rarely in healthy control subjects[7]. Further investigations of peripheral blood leukocytes or bone marrow cells from severe invasive GAS patients are required, to clarify whether the human counterpart of γIMCs is a major source of IFN-γ in STSS patients.

PMNs are known to be essential for protection against non-invasive streptococcal infections. Following infection with severe invasive strains, PMNs are impaired by enhanced virulence factors (for example, streptolysin O)[18,27], and therefore other protective mechanisms are required for the recovery. The results of our present study indicate that γIMCs, a novel class of differentiated granulocytic ring cells, which comprise the major source of IFN-γ during the early phase of severe invasive GAS infections, may have an important role. During the later stage of infection, IFN-γ derived from T cells and NK cells may be detrimental to the host. Nevertheless, we believe that the orchestrated regulation of γIMCs serves as a protective mechanism against severe invasive bacterial infections.

Methods

Bacterial strains. The STSS criteria in this study are based on those proposed by the Working Group on Severe Streptococcal Infections[44]. The clinical isolates from STSS (NIH34 (*emm3* genotype], NIH230 (*emm49* genotype), NIH186 (*emm1* genotype), and NIH202-2 (*emm1* genotype)), and also from non-invasive infections (K33 (*emm3* genotype)), were collected by the Working Group for Beta-hemolytic Streptococci in Japan[18,27].

Mice. All work performed using mice was carried out in accordance with the guidelines for animal care approved by National Institute of Infectious Diseases. C3H/HeN and C57BL/6 mice (male, 5–6-weeks-old) were purchased from SLC. C57BL/6.*Rag1*$^{-/-}$ (ref. 26) and C57BL/6.*Ifng*$^{-/-}$ (ref. 45) mice were purchased from the Jackson Laboratory. All mice were maintained in a specific pathogen-free condition.

GAS infections in a mouse model. GAS were grown to late-log phase (OD_{600} = 0.75–0.95). Then, 1.0×10^7 CFU to 5.0×10^7 CFU GAS, suspended in 0.5 ml PBS, were i.p. inoculated into 6–8-week-old male mice. In some experiments, mice were i.p. administered with 1 mg of an anti-mouse IFN-γ neutralizing mAb (clone R4-6A2) or control rat IgG, or 10 ng of recombinant mouse IFN-γ (Wako Pure Chemical Industries) at infection. Plasma production of CXCL10 (an IFN-γ-inducible protein) at 24 h, after NIH34 infection, was used to assess the activity of inoculated IFN-γ (10 ng per mouse) in *Ifng*$^{-/-}$ recipients (*Ifng*$^{-/-}$ mice, $230.1\pm58.2\,pg\,ml^{-1}$; IFN-γ-treated *Ifng*$^{-/-}$ mice, $468.2\pm147.2\,pg\,ml^{-1}$*; C57BL/6 mice as positive control, $460.6\pm126.9\,pg\,ml^{-1}$*). Data were expressed as mean ± s.d. ($n=5$). The differences compared with *Ifng*$^{-/-}$ mice were statistically significant ($^*P<0.05$) as determined by Student's *t*-test. Survival curves were compared using a log-rank test.

Measurement of cytokines in plasma. The plasma cytokine levels were determined by FlowCytomix (eBioscience) using a FACSCalibur flow cytometer (Becton, Dickinson and Company (BD)), according to the manufacturer's instructions.

Flow cytometry analysis. For the *in vivo* ICS assay[22,23], at day 2 post-infection, mice were intravenously (i.v.) injected with 500 µl of a PBS solution containing 100 µg monensin (Sigma-Aldrich) at 6 h before collecting. Splenocytes, peripheral blood cells, bone marrow cells, and leukocytes in the peritoneal cavity, kidney, and skin were collected and rapidly processed on ice. Single-cell suspensions were prepared, and red blood cells were removed using an ammonium chloride lysis buffer. For the *in vitro* ICS assay, non-infected or infected cells were cultured with $10\,\mu g\,ml^{-1}$ brefeldin A (Sigma-Aldrich) for 3 h. One million cells were stained with Alexa Fluor 488-, FITC-, PE-, Alexa Fluor 647-, allophycocyanin (APC)-,or Pacific Blue-conjugated Abs (clones and suppliers, Supplementary Table S2) at 4 °C for 15 min. Nonspecific staining was blocked with an anti-mouse FcγR mAb (clone 2.4G2). Dead cells were excluded by 7-aminoactinomycin D (7-AAD; Sigma-Aldrich) staining. After washing, cells were fixed in 2% paraformaldehyde/PBS for 10 min and then permeabilized in 0.5% saponin/0.5% BSA/PBS (permeabilization

buffer), before being stained with a PE- or APC-conjugated anti-mouse IFN-γ mAb (clone XMG1.2; eBioscience) or isotype control Ab (eBioscience) for 45 min at 4 °C. Cells were washed, first with permeabilization buffer, then with FACS buffer, before being applied to a FACSCalibur or FACSAria flow cytometer (BD). Analyses were performed using FlowJo software (Ashland, OR).

Cytological analysis. Fifty thousand cells were subjected to a cytospin (Thermo Shandon). For morphological analysis, the cytospin preparations were fixed with methanol and visualized with May-Grünwald-Giemsa staining. For intracellular IFN-γ staining, the cytospin preparations were fixed with 2% paraformaldehyde for 10 min, treated with 50 mM NH_4Cl/PBS for 15 min, and blocked with an anti-mouse FcγR mAb (clone 2.4G2) in permeabilization buffer for 15 min. Slides were stained with an APC-conjugated anti-mouse IFN-γ mAb (clone XMG1.2) or isotype control Ab (eBioscience) for 45 min, washed 3 times with permeabilization buffer, and then washed 3 times with PBS. Nuclei were visualized with propidium iodide staining. Samples were viewed and photographed with a Carl Zeiss LSM510 confocal laser scanning microscope.

Histology. For histological analysis, the tissues from GAS-infected mice were fixed in 10% formalin/PBS. The paraffin-embedded sections were stained with hematoxylin and eosin.

***In vitro* culture of γIMCs and BMPCs**. Purified $CD11b^+$ $CD11c^-$ $F4/80^{low}$ $Ly\text{-}6G^+$ γIMCs and $CD11b^+$ $CD11c^{low}$ $F4/80^+$ $Ly\text{-}6G^{low}$ BMPCs from GAS-infected (monensin-untreated) mice were cultured at 0.5×10^6 cells per ml in medium containing RPMI 1640 (Wako) with 10% FBS (Nichirei), 100 U ml^{-1} penicillin, 10 μg ml^{-1} streptomycin, 2 mM glutamine, 25 mM HEPES, and 50 μM 2-ME, with or without 10–50 ng ml^{-1} recombinant mouse GM-CSF, G-CSF, M-CSF, or IL-5 (R&D Systems), in the presence or absence of 1 μg ml^{-1} control rat IgG or R4-6A2, for 2–6 days. On days 2 and 4, 50% of the medium was replaced with fresh medium, or the cells were collected for May-Grünwald-Giemsa staining and flow cytometry analysis. In some experiments, the cells were cultured at 0.5×10^6 cells ml^{-1} with 25 μg ml^{-1} erythromycin and NIH34 (MOI 100) in 10% FBS/phenol red-free RPMI medium, supplemented with 10 ng ml^{-1} GM-CSF, in the presence of 1 μg ml^{-1} control rat IgG or R4-6A2 for 24 h. The levels of IFN-γ and NO in the culture supernatants were measured by an instant ELISA kit (eBioscience) and a Griess reagent (Wako), respectively, according to the manufacturer's instructions.

***In vitro* culture of Eos and MDSCs**. For obtaining Eos, naïve bone marrow cells were cultured in 10% FBS/RPMI medium supplemented with stem cell factor (PeproTech) and FLT3-ligand (PeproTech) for 4 days, and then with medium containing recombinant mouse IL-5 (R&D Systems). On day 12, the cells were collected for May-Grünwald-Giemsa staining and flow cytometry analysis[46]. To isolate bone marrow-derived MDSCs, naïve bone marrow cells were cultured at 1.0×10^6 cells per ml in 10% FBS/RPMI medium, supplemented with 40 ng ml^{-1} GM-CSF. On day 4, the cells were collected for FACS analysis of $CD11b^+$ $CD11c^-$ $Ly\text{-}6C^+$ $Ly\text{-}6G^{low}$ MDSCs[9].

Ag-specific T-cell proliferation and IFN-γ production. The Ag-specific proliferation of $CD8^+$ T cells was evaluated using OT-I OVA-specific MHC Class I-restricted TCR transgenic mice. Varying amounts of purified $CD11b^+$ $CD11c^-$ $F4/80^{low}$ $Ly\text{-}6G^+$ γIMCs from infected C57BL/6 mice at 2 days post-infection, or bone marrow-derived $F4/80^+$ $Ly\text{-}6C^+$ $Ly\text{-}6G^{low}$ MDSCs, were added to 2.0×10^5 naïve splenocytes from OT-I mice in medium containing RPMI 1640 with 10% FBS in a U-bottom 96-well plate. These co-cultures were stimulated with antigenic $OVA_{357-364}$ peptides (10 μM) for 4 days. Proliferation of OT-I cells in triplicate was estimated by the incorporation of [^{3}H] thymidine (1 μCi (0.0037 MBq) per well), added at 18 h before cell harvest. The level of IFN-γ in the culture supernatants was measured by an instant ELISA kit (eBioscience), according to the manufacturer's instructions.

Adoptive transfer of γIMCs. $CD11b^+$ $CD11c^-$ $F4/80^{low}$ $Ly\text{-}6G^+$ γIMCs in splenocytes from *Ifng*$^{+/+}$ mice infected with NIH34 (3.0×10^7 CFU) for 48 h were isolated with a FACSAria flow cytometer. Recipient mice were i.v. administered with purified $CD11b^+$ $CD11c^-$ $F4/80^{low}$ $Ly\text{-}6G^+$ γIMCs (3.0×10^6 cells), and i.p. inoculated with NIH34 (1.0×10^7 CFU to 5.0×10^7 CFU) on the same day.

Measurement of bacterial loads. At 24 h post-infection, 20 μl of peripheral blood was removed from the tail vein by phlebotomy. The blood was diluted at 1:10–1:1000 with PBS and spread on a Columbia agar plate containing 5% sheep blood (BD). To determine the number of NIH34 in peripheral blood, the plates were incubated for 20 h at 37 °C in a 5% CO_2 atmosphere, and the colonies were counted. The number of NIH34 was compared statistically using the Mann-Whitney *U*-test.

References

1. Lappin, E. & Ferguson, A. J. Gram-positive toxic shock syndromes. *Lancet Infect. Dis.* **9,** 281–290 (2009).
2. Cunningham, M. W. Pathogenesis of group A streptococcal infections. *Clin. Microbiol. Rev.* **13,** 470–511 (2000).
3. Davies, H. D *et al.* Invasive group A streptococcal infections in Ontario, Canada. Ontario Group A Streptococcal Study Group. *N. Engl. J. Med.* **335,** 547–554 (1996).
4. Bisno, A. L. & Stevens, D. L. Streptococcal infections of skin and soft tissues. *N. Engl. J. Med.* **334,** 240–245 (1996).
5. Raeder, R. H., Barker-Merrill, L., Lester, T., Boyle, M. D. & Metzger, D. W. A pivotal role for interferon-gamma in protection against group A streptococcal skin infection. *J. Infect. Dis.* **181,** 639–645 (2000).
6. Stavem, P., Hjort, P. F., Vogt, E. & van der Hagen, C. B. Ring-shaped nuclei of granulocytes in a patient with acute erythroleukaemia. *Scand. J. Haematol.* **6,** 31–32 (1969).
7. Langenhuijsen, M. M. Neutrophils with ring-shaped nuclei in myeloproliferative disease. *Br. J. Haematol.* **58,** 227–230 (1984).
8. Biermann, H. *et al.* Murine leukocytes with ring-shaped nuclei include granulocytes, monocytes, and their precursors. *J. Leukoc. Biol.* **65,** 217–231 (1999).
9. Rossner, S. *et al.* Myeloid dendritic cell precursors generated from bone marrow suppress T cell responses via cell contact and nitric oxide production *in vitro*. *Eur. J. Immunol.* **35,** 3533–3544 (2005).
10. Dardalhon, V. *et al.* Tim-3/galectin-9 pathway: regulation of Th1 immunity through promotion of CD11b+Ly-6G+ myeloid cells. *J. Immunol.* **185,** 1383–1392 (2010).
11. Movahedi, K. *et al.* Identification of discrete tumor-induced myeloid-derived suppressor cell subpopulations with distinct T cell-suppressive activity. *Blood* **111,** 4233–4244 (2008).
12. Youn, J. I., Nagaraj, S., Collazo, M. & Gabrilovich, D. I. Subsets of myeloid-derived suppressor cells in tumor-bearing mice. *J. Immunol.* **181,** 5791–5802 (2008).
13. Ribechini, E., Greifenberg, V., Sandwick, S. & Lutz, M. B. Subsets, expansion and activation of myeloid-derived suppressor cells. *Med. Microbiol. Immunol.* **199,** 273–281 (2010).
14. Medina, E., Goldmann, O., Rohde, M., Lengeling, A. & Chhatwal, G. S. Genetic control of susceptibility to group A streptococcal infection in mice. *J. Infect. Dis.* **184,** 846–852 (2001).
15. Goldmann, O., Chhatwal, G. S. & Medina, E. Immune mechanisms underlying host susceptibility to infection with group A streptococci. *J. Infect. Dis.* **187,** 854–861 (2003).
16. Goldmann, O. *et al.* The role of the MHC on resistance to group a streptococci in mice. *J. Immunol.* **175,** 3862–3872 (2005).
17. Goldmann, O., Chhatwal, G. S. & Medina, E. Contribution of natural killer cells to the pathogenesis of septic shock induced by Streptococcus pyogenes in mice. *J. Infect. Dis.* **191,** 1280–1286 (2005).
18. Ikebe, T. *et al.* Highly frequent mutations in negative regulators of multiple virulence genes in group A streptococcal toxic shock syndrome isolates. *PLoS Pathog.* **6,** e1000832 (2010).
19. Arad, G., Levy, R., Hillman, D. & Kaempfer, R. Superantigen antagonist protects against lethal shock and defines a new domain for T-cell activation. *Nat. Med.* **6,** 414–421 (2000).
20. Norrby-Teglund, A. *et al.* Evidence for superantigen involvement in severe group a streptococcal tissue infections. *J. Infect. Dis.* **184,** 853–860 (2001).
21. Kotb, M. *et al.* An immunogenetic and molecular basis for differences in outcomes of invasive group A streptococcal infections. *Nat. Med.* **8,** 1398–1404 (2002).
22. Liu, F. & Whitton, J. L. Cutting edge: re-evaluating the *in vivo* cytokine responses of CD8+ T cells during primary and secondary viral infections. *J. Immunol.* **174,** 5936–5940 (2005).
23. Sun, J., Madan, R., Karp, C. L. & Braciale, T. J. Effector T cells control lung inflammation during acute influenza virus infection by producing IL-10. *Nat. Med.* **15,** 277–284 (2009).
24. Nooh, M. M., El-Gengehi, N., Kansal, R., David, C. S. & Kotb, M. HLA transgenic mice provide evidence for a direct and dominant role of HLA class II variation in modulating the severity of streptococcal sepsis. *J. Immunol.* **178,** 3076–3083 (2007).
25. Abdeltawab, N. F. *et al.* An unbiased systems genetics approach to mapping genetic loci modulating susceptibility to severe streptococcal sepsis. *PLoS Pathog.* **4,** e1000042 (2008).
26. Mombaerts, P. *et al.* RAG-1-deficient mice have no mature B and T lymphocytes. *Cell* **68,** 869–877 (1992).
27. Ato, M., Ikebe, T., Kawabata, H., Takemori, T. & Watanabe, H. Incompetence of neutrophils to invasive group A streptococcus is attributed to induction of plural virulence factors by dysfunction of a regulator. *PLoS One* **3,** e3455 (2008).
28. Eriksson, B. K., Andersson, J., Holm, S. E. & Norgren, M. Epidemiological and clinical aspects of invasive group A streptococcal infections and the streptococcal toxic shock syndrome. *Clin. Infect. Dis.* **27,** 1428–1436 (1998).
29. Iwasaki, H. *et al.* Identification of eosinophil lineage-committed progenitors in the murine bone marrow. *J. Exp. Med.* **201,** 1891–1897 (2005).

30. Angulo, I. *et al.* Involvement of nitric oxide in bone marrow-derived natural suppressor activity. Its dependence on IFN-gamma. *J. Immunol.* **155,** 15–26 (1995).
31. Angulo, I. *et al.* Early myeloid cells are high producers of nitric oxide upon CD40 plus IFN-gamma stimulation through a mechanism dependent on endogenous TNF-alpha and IL-1alpha. *Eur. J. Immunol.* **30,** 1263–1271 (2000).
32. Pelaez, B., Campillo, J. A., Lopez-Asenjo, J. A. & Subiza, J. L. Cyclophosphamide induces the development of early myeloid cells suppressing tumor cell growth by a nitric oxide-dependent mechanism. *J. Immunol.* **166,** 6608–6615 (2001).
33. Campillo, J. A., Pelaez, B., Angulo, I., Bensussan, A. & Subiza, J. L. Involvement of IFNbeta on IFNgamma and nitric oxide (NO) production by bone marrow (BM) cells in response to lipopolysaccharide. *Biomed. Pharmacother.* **60,** 541–547 (2006).
34. Gallina, G. *et al.* Tumors induce a subset of inflammatory monocytes with immunosuppressive activity on CD8+ T cells. *J. Clin. Invest.* **116,** 2777–2790 (2006).
35. Belyaev, N. N. *et al.* Induction of an IL7-R(+)c-Kit(hi) myelolymphoid progenitor critically dependent on IFN-gamma signaling during acute malaria. *Nat. Immunol.* **11,** 477–485 (2010).
36. Serbina, N. V., Jia, T., Hohl, T. M. & Pamer, E. G. Monocyte-mediated defense against microbial pathogens. *Annu. Rev. Immunol.* **26,** 421–452 (2008).
37. Metcalf, D. & Nicola, N. A. Proliferative effects of purified granulocyte colony-stimulating factor (G-CSF) on normal mouse hemopoietic cells. *J. Cell. Physiol.* **116,** 198–206 (1983).
38. Hitoshi, Y. *et al.* Distribution of IL-5 receptor-positive B cells. Expression of IL-5 receptor on Ly-1(CD5)+ B cells. *J. Immunol.* **144,** 4218–4225 (1990).
39. Lee, J. J. & McGarry, M. P. When is a mouse basophil not a basophil? *Blood* **109,** 859–861 (2007).
40. Delano, M. J. *et al.* MyD88-dependent expansion of an immature GR-1(+) CD11b(+) population induces T cell suppression and Th2 polarization in sepsis. *J. Exp. Med.* **204,** 1463–1474 (2007).
41. Zhan, Y., Lieschke, G. J., Grail, D., Dunn, A. R. & Cheers, C. Essential roles for granulocyte-macrophage colony-stimulating factor (GM-CSF) and G-CSF in the sustained hematopoietic response of Listeria monocytogenes-infected mice. *Blood* **91,** 863–869 (1998).
42. Baldridge, M. T., King, K. Y., Boles, N. C., Weksberg, D. C. & Goodell, M. A. Quiescent haematopoietic stem cells are activated by IFN-gamma in response to chronic infection. *Nature* **465,** 793–797 (2010).
43. Trottier, M. D., Newsted, M. M., King, L. E. & Fraker, P. J. Natural glucocorticoids induce expansion of all developmental stages of murine bone marrow granulocytes without inhibiting function. *Proc. Natl Acad. Sci. USA* **105,** 2028–2033 (2008).
44. Breiman, R. F. *et al.* Defining the group A streptococcal toxic shock syndrome. Rationale and consensus definition. *JAMA* **269,** 390–391 (1993).
45. Dalton, D. K. *et al.* Multiple defects of immune cell function in mice with disrupted interferon-gamma genes. *Science* **259,** 1739–1742 (1993).
46. Dyer, K. D. *et al.* Functionally competent eosinophils differentiated *ex vivo* in high purity from normal mouse bone marrow. *J. Immunol.* **181,** 4004–4009 (2008).

Acknowledgements

We thank Dr. Satoshi Takaki (Research Institute National Center for Global Health and Medicine) and Dr. Kiyoshi Takatsu (University of Toyama) for providing the anti-IL-5Rα mAb (clone H7); Dr. Akihiko Yoshimura (Keio University) for providing the anti-IFN-γ mAb; Dr. Hideki Fujii and Dr. Shigeo Koyasu (Keio University) for providing the OT-I transgenic mice; Dr. Paul M. Kaye (University of York) for critical comments; and Ms Yoko Nakamura for technical assistance. This work was partly supported by a grant (H22-Shinkou-Ippan-013 to M.A., T.I., and H.W.) from the Ministry of Health, Labour and Welfare of Japan, and by a Grant-in-Aid for Young Scientists (B) (22790959 to T.M.) from the Japan Society for the Promotion of Science.

Author contributions

T.M., M.A., and T.I. designed and performed the experiments. T.M. and M.A. analysed the data. T.M., M.A., T.I., M.O., H.W. and K.K. wrote the manuscript.

Additional information

Supplementary Information accompanies this paper at http://www.nature.com/naturecommunications

Competing financial interests: The authors declare no competing financial interests.

Reprints and permission information is available online at http://npg.nature.com/reprintsandpermissions/

How to cite this article: Matsumura, T. *et al.* Interferon-γ-producing immature myeloid cells confer protection against severe invasive group A *Streptococcus* infections *Nat. Commun.* 3:678 doi: 10.1038/ncomms1677 (2012).

Jpn. J. Infect. Dis., 65, 19-27, 2012

Original Article

Newly Established Monoclonal Antibodies for Immunological Detection of H5N1 Influenza Virus

Kazuo Ohnishi[1], Yoshimasa Takahashi[1], Naoko Kono[2], Noriko Nakajima[3], Fuminori Mizukoshi[1], Shuhei Misawa[4], Takuya Yamamoto[1], Yu-ya Mitsuki[1], Shu-ichi Fu[1], Nakami Hirayama[1], Masamichi Ohshima[1], Manabu Ato[1], Tsutomu Kageyama[2], Takato Odagiri[2], Masato Tashiro[2], Kazuo Kobayashi[1], Shigeyuki Itamura[2], and Yasuko Tsunetsugu-Yokota[1]*

[1]Department of Immunology, [2]Influenza Virus Research Center, and [3]Department of Pathology, National Institute of Infectious Diseases, Tokyo 162-8640; and [4]Tsuruga Institute of Biotechnology, Toyobo, Co., Ltd., Fukui 914-8550, Japan

(Received October 4, 2011. Accepted October 28, 2011)

SUMMARY: The H5N1 subtype of the highly pathogenic (HP) avian influenza virus has been recognized for its ability to cause serious pandemics among humans. In the present study, new monoclonal antibodies (mAbs) against viral proteins were established for the immunological detection of H5N1 influenza virus for research and diagnostic purposes. B-cell hybridomas were generated from mice that had been hyperimmunized with purified A/Vietnam/1194/2004 (NIBRG-14) virion that had been inactivated by UV-irradiation or formaldehyde. After screening over 4,000 hybridomas, eight H5N1-specific clones were selected. Six were specific for hemagglutinin (HA) and had in vitro neutralization activity. Of these, four were able to broadly detect all tested clades of the H5N1 strains. Five HA-specific mAbs detected denatured HA epitope(s) in Western blot analysis, and two detected HP influenza virus by immunofluorescence and immunohistochemistry. A highly sensitive antigen-capture sandwich ELISA system was established by combining mAbs with different specificities. In conclusion, these mAbs may be useful for rapid and specific diagnosis of H5N1 influenza. Therapeutically, they may have a role in antibody-based treatment of the disease.

INTRODUCTION

The highly pathogenic (HP) H5N1 avian influenza virus caused the first outbreak in humans in Hong Kong in 1997. This outbreak resulted in the infection of 18 people and resulted in six deaths (1,2). Thereafter, it was determined that H5N1 avian influenza virus was continuously circulated among geese in Southeastern China. Eventually, it spread to other Southeast Asian countries, where it severely damaged poultry farms (3,4). Subsequent H5N1 outbreaks in humans occurred in China and Vietnam in 2003 and in Indonesia in 2005. The most recent endemic has occurred in Egypt. According to a World Health Organization report, the H5N1 avian influenza virus had infected 565 people and resulted in 331 deaths by August 19, 2011 (5). Therefore, although sporadic, this fatal human infection is persistent and has the potential to cause serious future pandemics.

In humans, infection with HP H5N1 avian influenza virus causes high fever, coughing, shortness of breath, and radiological findings of pneumonia (6–8). In severe cases, rapidly progressive bilateral pneumonia develops, causing respiratory failure and may be responsible for the high mortality associated with this virus. de Jong et al. analyzed human cases of H5N1 infection and found that a high viral load and the resulting intense inflammatory response caused severe symptoms; furthermore, viral RNA was frequently detected in the rectum, blood, and nasopharynx (9). Thus, it is essential to detect HP influenza virus infection early and rapidly in order to provide early interventions that protect patients from devastating respiratory failure that arises from a high viral load. Additionally, early viral detection would facilitate rapid identification of infected patients and prevent unregulated contact with other people.

The present diagnostic standard for HP H5N1 influenza is the presence of the neutralization antibody. However, it takes more than 1 week for H5N1-specific antibodies to develop, and a well-equipped biosafety level 3 (BSL3) laboratory is required for the virus neutralization assay. A simpler method is the hemagglutination-inhibition assay using horse erythrocyte. This method has been widely performed on paired acute and convalescent sera from patients with HP H5N1 influenza virus infections. Although this method has acceptable sensitivity, its specificity has been questioned (7).

Isolating the virus from patient samples is the gold standard for diagnosing an infection; however, this is not always possible. For example, the method of sample preparation and preservation strongly influence the ability to isolate the virus. Moreover, a BSL3 laboratory is essential. At present, the most sensitive and rapid method for initial diagnosis of H5N1 virus infections is by conventional or real-time reverse-transcriptase polymerase chain reaction (RT-PCR). However, this proce-

*Corresponding author: Mailing address: Department of Immunology, National Institute of Infectious Diseases, Toyama 1-23-1, Shinjuku-ku, Tokyo 162-8640, Japan. Tel: +81-3-5285-1111, Fax: +81-5285-1150, E-mail: yyokota@nih.go.jp

dure requires expertise in molecular virology and expensive equipment and reagents. Moreover, because of its high sequence specificity, this approach could fail to identify mutant influenza viruses that continually evolve due to a high mutation rate (8).

For screening suspected H5N1 influenza virus in the field, the ideal approach would be to employ an immunology-based technique that detects viral antigens. Such a method is simple and rapid. However, its sensitivity and specificity depend highly on the antibodies used. Thus, an immunological assay that uses appropriate specific antibodies against H5N1 in combination with specific antibodies against other subtypes of influenza virus or viruses that cause febrile diseases would be useful for screening in areas with endemic influenza-like illness. While there are several rapid influenza virus diagnostic systems available for seasonal influenza (10), few exist for H5N1 influenza. Therefore, we have developed a simple and rapid diagnostic system with high sensitivity and specificity for H5N1 influenza virus.

Influenza virus belongs to the family *Orthomyxoviridae*; its genome consists of a negative-sense, single-stranded RNA with eight segments, each encoding structural and non-structural proteins (11). Influenza A viruses are classified into several subtypes based on the hemagglutinin (HA) and neuraminidase (NA) serotypes. In total, there are 16 HA and 9 NA serotypes. The H5N1 viruses are divided into clades 1 and 2 based on their HA genotypes. Clade 2 has been further subdivided into five sub-clades (12). Clade 1 viruses were predominant in Vietnam, Thailand, and Cambodia in the early phase of the 2004–2005 outbreak, whereas clade 2.1 viruses were endemic in Indonesia at that time (8). These two viruses are the major prototypes for the preparation of prepandemic H5N1 vaccines. We used inactivated purified clade 1 virion [A/Vietnam/1194/2004 (NIBRG-14)] as an immunizing antigen to establish mouse monoclonal antibodies (mAbs) specific for H5N1 influenza virus. Characterization of these mAbs revealed that they could detect H5N1 viruses when used in an immunofluorescence staining assay (IFA), Western blotting analysis, immunohistochemistry, and antigen-capture sandwich ELISA. In addition, the mAbs had significant in vitro neutralization activity against H5N1 viruses, and some broadly detected both clade 1 and 2 viruses.

MATERIALS AND METHODS

Viruses and cell culture: The NIBRG-14 (H5N1) virus, which possesses modified HA and NA genes derived from the A/Vietnam/1194/2004 strain on the backbone of six internal genes of A/Puerto Rico/8/34 (PR8), was provided by the National Institute for Biological Standards and Controls (NIBSC; Potters Bar, UK). A/Indonesia/05/2005 (Indo5/PR-8-RG2), A/Turkey/1/2005 (NIBRG-23), A/Anhui/01/2005 (Anhui01/PR8-RG5) were also obtained from NIBSC. All non-H5N1 strains were obtained from a stockpile of seed vaccines of the Influenza Virus Research Center of the National Institute of Infectious Diseases. The live virus was manipulated in a BSL2 laboratory. To produce and purify the virion, the NIBRG-14 and PR8 viruses were propagated in the allantoic cavity of 10-day-old embryonated hens' eggs and purified through a 10–50% discontinuous sucrose gradient by ultracentrifugation (13). The viruses were then resuspended in phosphate-buffered saline (PBS) and inactivated by ultraviolet (UV) irradiation or by treatment with 0.05% formalin at 4°C for 2 weeks. These preparations were served as the inactivated H5N1 virus fraction. These conditions have been previously shown to completely inactivate H5N1 viruses.

Production of mAbs: Nine-week-old female BALB/c mice (Japan SLC, Shizuoka, Japan) were immunized subcutaneously with 20 μg of UV- or formaldehyde-inactivated NIBRG-14 (H5N1) virus using Freund's Complete Adjuvant (Sigma, St. Louis, Mo., USA). Two weeks later, the mice were boosted with a subcutaneous injection of 5 μg of the inactivated virus emulsified with Freund's Incomplete Adjuvant (Sigma). Three days after the boost, sera from the mice were tested by ELISA to determine the antibody titer against the NIBRG-14 virus. The three mice with the highest antibody titers were given an additional boost 14 days after the first boost by intravenous injection of 5 μg of the inactivated virus. Three days later, the spleens of these three mice were excised, and the spleen cells were fused with Sp2/O-Ag14 myeloma cells using the polyethylene glycol method of Kozbor and Roder (14). The fused cells were cultured on twenty 96-well plates and selected with hypoxiantine-aminopterin-thymidine (HAT) medium. The first screening was conducted by ELISA using formalin-inactivated purified NIBRG-14 (H5N1) and PR-8 (H1N1) virions, which were lysed with 1% Triton X100. The lysates (1 mg/ml) were diluted 2,000-fold with ELISA-coating buffer (50 mM sodium bicarbonate, pH 9.6), and the ELISA plates (Dynatech, Chantily, Va., USA) were coated at 4°C overnight. After blocking with 1% ovalbumin in PBS-Tween (10 mM phosphate buffer, 140 mM NaCl, 0.05% Tween 20, pH 7.5) for 1 h, the culture supernatants of the HAT-selected hybridomas were added and incubated for 1 h. After washing with PBS-Tween, the bound antibodies were detected using alkaline phosphatase-conjugated anti-mouse IgG (1:2,000; Zymed, South San Francisco, Calif., USA) and *p*-nitrophenyl phosphate, which served as a substrate. In this first screening, hybridomas that reacted to the H5N1 virus (NIBRG-14) but not to the H1N1 virus (PR-8) were selected.

Baculoviral expression of recombinant HA and NA: Recombinant HA (rHA) and NA (rNA) proteins were produced as previously described (13). Briefly, the HA- and NA-coding genes of NIBRG-14 were amplified by PCR to attach a 6x-His tag to the C terminus of HA and to the N terminus of NA. The amplified DNAs were then cloned into pBacPAK8 (Clontech, Mountain View, Calif., USA) and transfected into Sf-21 (*Spodoptera frugiperda*) insect cells. Recombinant baculoviruses containing the rHA and rNA genes were isolated were used to infect Sf-21 cells. The recombinant proteins tagged with 6x-His were purified with TALON columns (Clontech) according to the manufacturer's protocol.

Neutralization assay: For the neutralization assay, 100 $TCID_{50}$ of H5N1 virus, a standard tissue culture infectious dose for such assays, was incubated for 30 min at 37°C in the presence or absence of the purified mAbs, which had been serially diluted twofold. The viruses

were then added to MDCK cell cultures that had been grown to confluence in a 96-well microtiter plate. The virus strains used were A/Vietnam/1194/2004 (NIBRG-14) (H5N1) (clade 1), A/Indonesia/05/2005 (Ind05/PR8-RG2) (H5N1) (clade 2.1), A/Turkey/1/2005 (NIBRG-23) (H5N1) (clade 2.2), and A/Anhui/01/2005 (Anhui01/PR8-RG5) (H5N1) (clade 2.3). After 3–5 days, the cells were fixed with 10% formaldehyde and stained with crystal violet to visualize the cytopathic effects induced by the virus (15). Neutralization antibody titers were expressed as the minimum concentration of purified immunoglobulin that inhibited a cytopathic effect.

Western blot analysis: UV-inactivated purified H5N1 virus (0.5 μg/lane) was loaded on SDS-PAGE gels under reducing conditions. The proteins were then transferred to a PVDF membrane (Genetics, Tokyo, Japan). After blocking with BlockAce reagent (Snow Brand Milk Products Co., Tokyo, Japan), the membranes were detected with the mAbs or diluted sera (1:1,000) that had been obtained from mice immunized with UV-irradiated H5N1 virus. After washing, the membrane was reacted with the peroxidase-conjugated $F(ab')_2$ fragment of anti-mouse IgG (H + L) (1:20,000; Jackson ImmunoResearch, West Grove, Pa., USA), and the bands were visualized on X-ray film (Kodak, Rochester, N.Y., USA) with chemiluminescent reagents (Amersham Biosciences, Piscataway, N.J., USA).

Purification and biotinylation of mAbs: Hybridomas were grown in Hybridoma-SFM medium (Invitrogen, Carlsbad, Calif., USA) supplemented with recombinant IL-6, penicillin (100 U/mL), and streptomycin (100 μg/mL) (16). The culture supernatants were harvested, and 1/100 volume of 1 M Tris-HCl (pH 7.4) and 1/500 volume of 10% NaN_3 were applied directly on a Protein G-Sepharose 6B column (Amersham Biosciences). The column was washed with PBS and eluted with glycine/HCl (pH 2.8). After measuring the OD_{280} of the fractions, the protein-containing fractions were pooled, and an equal volume of saturated $(NH_4)_2SO_4$ was added. The precipitated proteins were dissolved in PBS, dialyzed against PBS, and stored at −20°C. The purified antibodies were biotinylated with sulfo-NHS-LC-biotin (Pierce, Rockford, Ill., USA) according to the manufacturer's protocol.

Antigen-capture ELISA: The purified antigen-capturing mAb was immobilized on a microplate (Immulon 2; Dynatech) by incubating 4 μg/mL of the mAb in 50 mM sodium bicarbonate buffer (pH 8.6) at 4°C overnight. The microplate was blocked with 1% BSA, washed with PBS-Tween, and reacted with serial dilutions of UV-inactivated purified H5N1 virus for 1 h at room temperature. After washing with PBS-Tween, biotinylated probing mAb (0.1 μg/mL) was added to the wells for 1 h at room temperature. After washing, horseradish peroxidase (HRP)-labeled streptavidin (Zymed) was added to the wells for 1 h at room temperature. After washing, 0.4 mg/mL *o*-phenylenediamine (OPD Sigma P-8412) in OPD Buffer (0.05 M citrate-phosphate buffer pH 5.0, 0.04% H_2O_2) or TMB(+) substrate (DAKO, Kyoto, Japan) was added. The reaction was stopped by adding 2N H_2SO_4, and the OD_{490} or OD_{450} was measured using a multi-well plate reader (Flow Laboratories Inc., Inglewood, Calif., USA).

Immunohistochemistry: Lung tissues were harvested from mice infected with A/Vietnam/1194/2004 (NIBRG-14) or A/HongKong/483/97 (HK483). In addition, autopsied lung tissues of patients infected with influenza virus (H1N1 or 2009 H1N1pdm) were used. Formaldehyde- or formalin-fixed paraffin-embedded lung tissue sections were deparaffinized with xylene and graded ethanol and then autoclaved in 0.1 M citrate-buffer (pH 6.0) at 121°C for 10 min to retrieve the antigens. Endogenous peroxidase was inactivated with 0.3% hydrogen peroxide for 30 min at room temperature. After blocking with M.O.M. blocking reagent (Vector laboratories, Burlingame, Calif., USA) or 5% goat serum, the sections were incubated with each of the mouse mAbs or rabbit polyclonal antibody against type A influenza nucleoprotein at 4°C overnight. After washing off the excess antibodies, the sections were incubated with HRP-labeled anti-mouse IgG followed by tyramide signal amplification system (Biotin-free catalyzed amplification system, CSAII; DAKO) or biotinylated anti-rabbit IgG followed by streptavidin/HRP (LSAB kit; DAKO). The labeled peroxidase activity was detected using diaminobenzidine (DAB; Dojin, Kumamoto, Japan) in 0.015% hydrogen peroxide/0.05 M Tris-HCl (pH 7.6). The sections were counterstained with hematoxylin.

RESULTS

Generation of H5N1-specific mAbs: To establish hybridomas that secrete mAbs specific for the H5N1 virus, BALB/c mice were immunized with the whole virion fraction of purified A/Vietnam/1194/2004 (NIBRG-14) virus. The virus had been inactivated by conventional formaldehyde-fixation or by UV-irradiation to avoid possible changes in antigenicity caused by aldehyde fixation. A standard immunization protocol was used, where mice were boosted twice at 2-week intervals with antigen emulsified first in Freund's Complete Adjuvant and then in Freund's Incomplete Adjuvant. Three days after the final boost, a cell suspension was prepared from the spleens of three immunized mice and fused with SP-2/O myeloma using a polyethylene-glycol method. The fused cells were then selected with HAT (14). Hybridoma screening yielded eight hybridoma clones that reacted to NIBRG-14 lysate but not PR-8 lysate in ELISA (Table 1). Of these clones, seven were from mice immunized with UV-inactivated virion, and one was from mice immunized with formaldehyde-inactivated virion. Six clones (Niid_H5A, Niid_H5B, Niid_H5C, Niid_H5D, Niid_H5E, and Niid_H5F) reacted to rHA protein from a H5N1 virus (recHA_H5N1), while one clone (Niid_N1A) reacted to rNA protein from a H5N1 virus (recNA_H5N1). The remaining clone (Niid_150KA) did not react to either recHA_H5N1 or recNA_H5N1 by ELISA but did react to a 150-kDa molecule on Western blot analysis (described below). Interestingly, seven of the eight clones were from the mice immunized with UV-inactivated virus. The eight hybridomas were successfully cloned by a repeated limiting-dilution method and adapted to a serum-free hybridoma culture medium. The purified antibodies from each clone were biotinylated and used for further experiments.

Table 1. Summary of the eight H5N1-specific mAbs generated in this study

Clone name	Old name	Ig-subclass	ELISA				Western blot	IFA	Histology	Neutralization (μg/mL)	Hemagglutination inhibition
			H5N1_ NIBRG-14	H1N1_ PR-8	recHA_ H5N1	recNA_ H5N1					
Niid_H5A[1)]	YH-1A1	IgG2a	+++	−	+	−	57 kDa	++		1.5 (Clade-dep)	−
Niid_H5B[1)]	YH-2F11	IgG2a	+++	−	+++	−	57 kDa			25	+
Niid_H5C[1)]	OM-A	IgG2a	+++	−	++	−	57 kDa		+(mo/hu)	12	
Niid_H5D[1)]	OM-B	IgG2a	+++	−	++	−	57 kDa		+(mo)	12	
Niid_H5E[1)]	OM-C	IgG2a	+++	−	++	−	57 kDa			12 (Clade-dep)	
Niid_H5F	AY-2C2	IgG1	+++	−	++	−	ND	++		6	−
Niid_N1A[1)]	YH-2D3	IgG2a	+++	−	−	+	ND	++			
Niid_150KA[1)]	OM-D	IgG1	+++	−	−	−	150 kDa	++			−

[1)]: Clones derived from mice immunized with UV-inactivated virus. The remaining clone is derived from a mouse immunized with formaldehyde-inactivated virus.

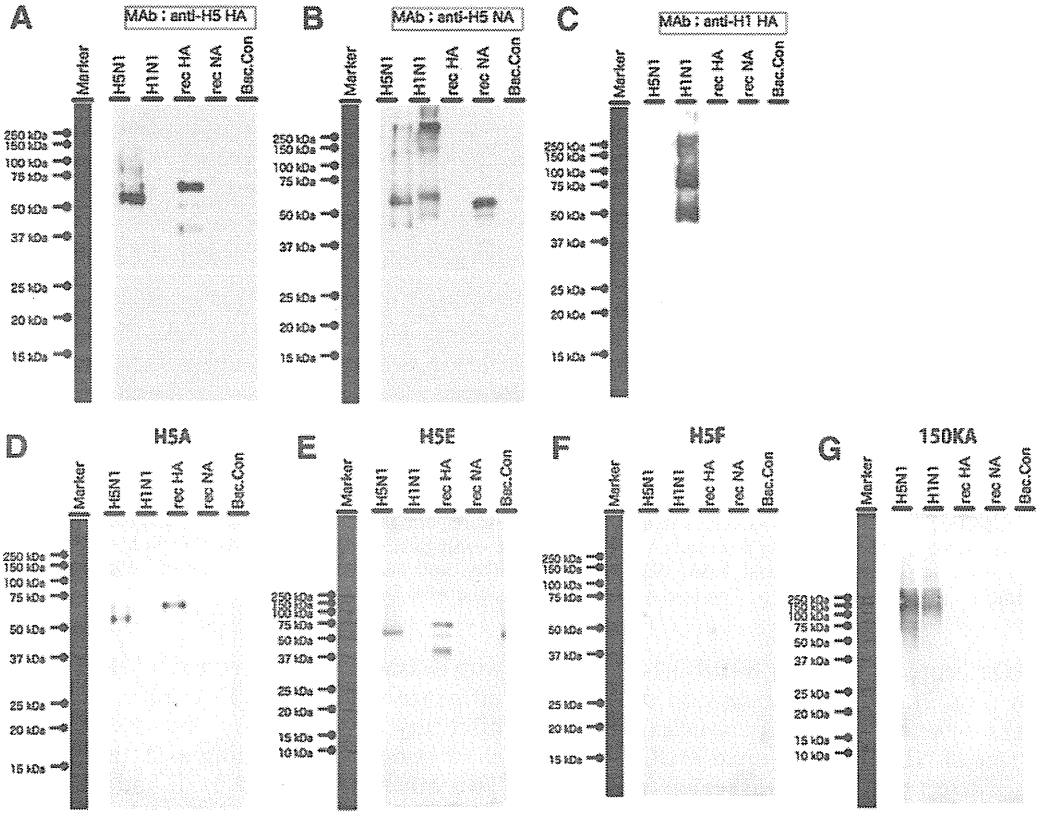

Fig. 1. Detection of influenza virus proteins in Western-blot analysis. Purified influenza virus proteins (0.5 μg/lane) were subjected to SDS-PAGE under reducing conditions. After blotting on a PVDF membrane, the proteins were detected by incubation with the eight monoclonal antibodies (mAbs), followed by incubation with the peroxidase-labeled $F(ab')_2$ fragment of donkey anti-mouse IgG. The mAbs were then visualized by chemiluminescent reaction. A, authentic anti-H5_hemagglutinin mAb; B, authentic anti-H5_neuraminidase mAb; C, authentic anti-H1_hemagglutinin mAb; D, Niid_H5A; E, Niid_H5E; F, Niid_H5F; G, Niid_150KA. The molecular weight markers are shown on the left.

Western blot analyses with the mAbs: Five mAbs (Niid_H5A, Niid_H5B, Niid_H5C, Niid_H5D, Niid_H5E) detected the 57-kDa H5_H1 protein by Western blot analysis, which suggests that the antibodies detected the linear epitope(s) of a HA1 fragment of H5_HA (Table 1 and Fig. 1). These antibodies also detected the 60-kDa recombinant H5-HA containing the His-tag. One of these clones, Niid_H5E, detected a 40-kDa subfragment of recombinant HA1, which suggests that the antigenic footprint detected by the mAb differs from that of the other four clones (Fig. 1). Niid-H5F, which reacted strongly to NIBRG-14 and rHA (H5) in ELISA, did not react to any proteins by Western blot analysis, presumably because the mAb detects a conformational epitope of H5-HA. The remaining clone, Niid_150KA, detected an unknown high molecular weight protein of approximately 150 kDa.

IFA with mAbs: Upon IFA, the HA-specific mAbs Niid-H5A and Niid_H5F, the NA-specific mAb Niid-N1A, and the Niid_150KA mAb that detects an

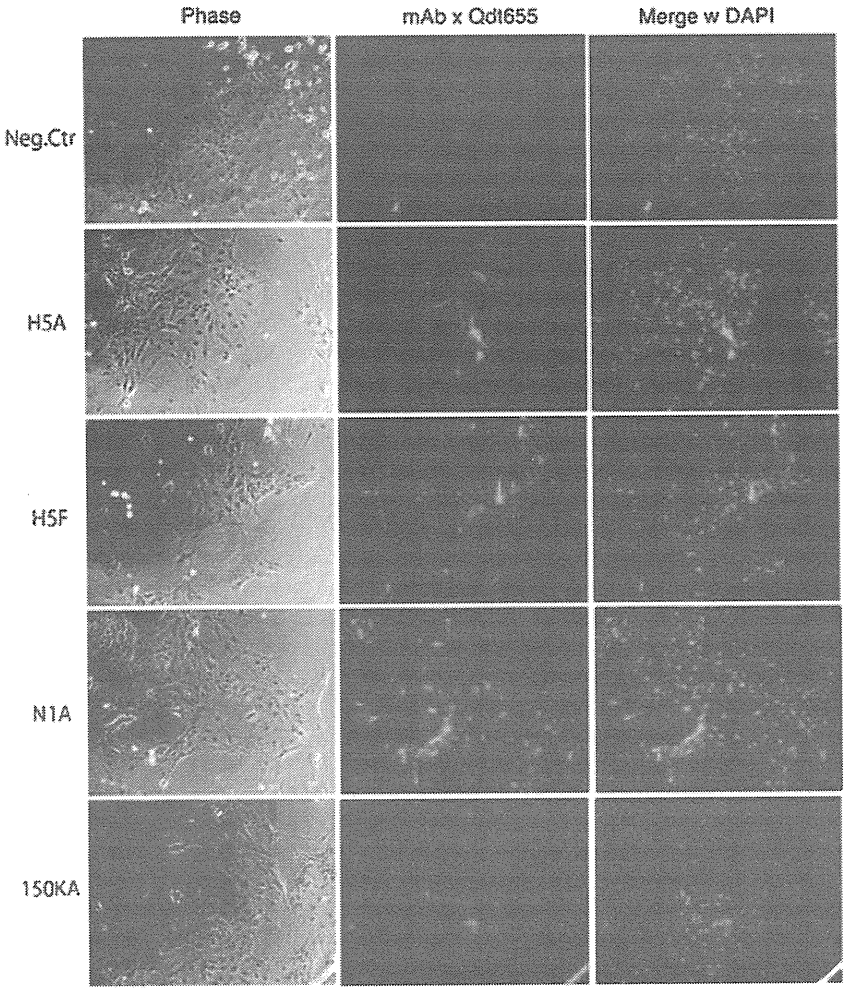

Fig. 2. Fluorescent immunostaining of H5N1 virus-infected MDCK cells with monoclonal antibodies (mAbs). Paraformaldehyde-fixed, H5N1 virus-infected MDCK cells were permeabilized by TBS-Tween and incubated with biotinylated mAbs. The mAbs were detected with Qdot655-conjugated streptavidin (red). Shown are representative staining patterns with Niid_H5A, Niid_H5F, Niid_N1A, and Niid_150KA. The negative control staining without mAb is shown on top. The nuclei were counterstained with DAPI (blue).

unknown 150-kDa protein bound to NIBRG-14-infected MDCK cells (Fig. 2). With the exception of Niid_H5F, these mAbs detected both the perinuclear region and the cell surface of NIBRG-14-infected MDCK cells. Niid_H5F did not detect the perinuclear region (presumably the Golgi body), which suggests that the antigenic footprint detected by this mAb differs from those of the other mAbs.

Immunohistochemistry: The Niid_H5C and Niid_H5D mAbs detected influenza virus antigens in the epithelial cells of the bronchioles and alveoli of 4% formaldehyde-fixed, paraffin-embedded lung tissue sections from mice infected with A/Vietnam/1194/2004 (NIBRG-14) (Fig. 3a). However, none of the mAbs detected influenza virus antigen in lung tissue sections from mice infected with A/HongKong/483/97 (HK483) (Fig. 3). In contrast, a polyclonal antibody against type A influenza nucleoprotein detected type A influenza virus nucleoprotein in the tissue sections from both the NIBRG-14- and HK483-infected mice (Fig. 3b, d). Thus, Niid_H5C and Niid_H5D specifically detected the HA antigen of A/Vietnam/1194/2004 (NIBRG-14). The specificity of these mAbs was then examined by using autopsied lung tissue sections from patients infected with seasonal influenza virus (H1N1) or 2009 pandemic influenza virus (2009H1N1pdm). Niid_H5C did not exhibit any crossreactivity, but the Niid_H5D mAb did show non-specific staining with the human lung section. Two other mAbs, Niid_H5B and Niid_N1A, were also subjected to such immunohistochemical analysis but did not show any reaction.

Neutralization assay with mAbs: The ability of the mAbs to neutralize several H5N1 influenza strains was then tested (Table 2). The four purified H5N1 virus strains, NIBRG-14, Indo-RG2, NIBRG-23, and Anhui-RG5, were diluted to 2–3 $\times$ 10^2 $TCID_{50}$/0.05 mL (Table 2, lower panel) and incubated with titrated amounts of anti-H5_HA mAbs. The remaining infectivity was then noted (Table 2, upper panel). Niid_H5A most potently neutralized the NIBRG-14 strain; it completely neutralized influenza virus infectivity at a concentration of 78 ng/mL. However, Niid_H5A was less potent in neutralizing the Indo-RG2 and Anhui-RG5 strains, which indicates that the neutralizing ability of this mAb was clade-dependent. In contrast, Niid_H5F and Niid_H5D exhibited relatively broad neutralizing abilities, since they neutralized all of the strains that were tested. Niid_H5C and Niid_H5E also showed characteristic clade-

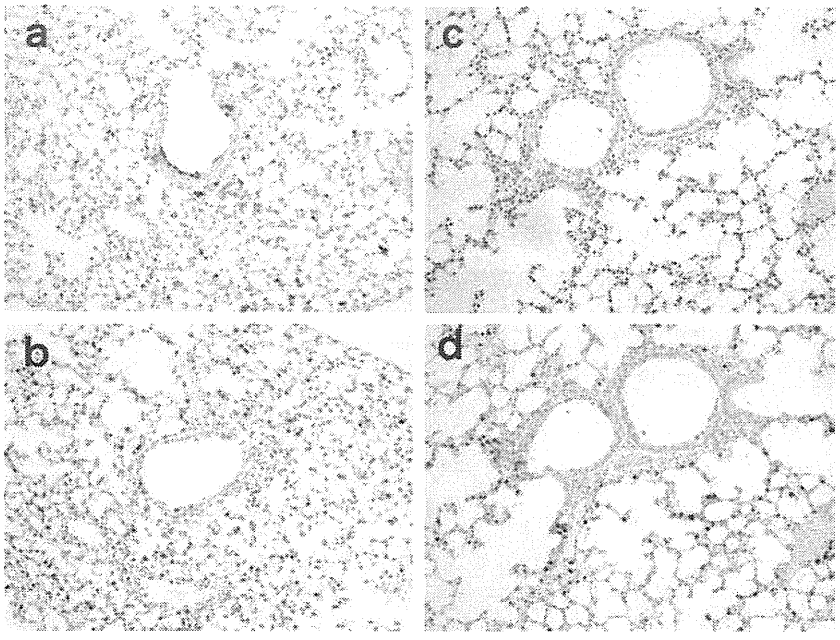

Fig. 3. Immunohistochemical analyses of lung sections from mice infected with A/Vietnam/1194/2004 (NIBRG-14) or A/HongKong/483/97 (HK483) virus. (a, b) Influenza virus antigens were detected in the epithelial cells of the bronchioles and alveoli of the mouse infected with A/Vietnam/1194/2004 (NIBRG-14) by the Niid_H5C clone (a) and polyclonal antibody against type A influenza nucleoprotein (b). (c, d) Virus antigens were not detected in the lung tissue section of the mouse infected with A/HongKong/483/97 (HK483) when Niid_H5C was used (c). However, virus antigens were detected in this section when a polyclonal antibody against type A influenza nucleoprotein was employed (d).

Table 2. Neutralizing ability of the eight mAbs generated in this study

Clone	Neutralizing antibody titer (ng/mL)			
	NIBRG-14 (clade 1)	Indo-RG2 (clade 2.1)	NIBRG-23 (clade 2.2)	Anhui-RG5 (clade 2.3)
Niid_H5A	78	>10,000	625	>10,000
Niid_H5C	625	625	313	>10,000
Niid_H5D	625	625	313	5,000
Niid_H5E	625	>10,000	>10,000	>10,000
Niid_H5F	313	313	156	2,500

Test no.	Virus infection index (Log_{10} $TCID_{50}$/0.05 mL)			
	NIBRG-14	Indo-RG2	NIBRG-23	Anhui-RG5
1	2.5	3.1	2.4	2.1
2	2.0	NT	2.0	2.4

The in vitro neutralization assay examined the ability of the mAbs to neutralize H5N1 virus infection of cultured MDCK cells. Briefly, purified H5N1 virus was diluted to 2–3 × 10^2 $TCID_{50}$/0.05 mL (the quantities are shown in the lower table) and incubated with serially-titrated purified mAbs for 1 h at 37°C. The samples were then placed into 96-well plates in which MDCK cells had been grown to 90% confluence. After 48 h, the cytotoxicity of the mAb-treated viruses was visualized by staining the cells with crystal violet.
NT, not tested.

dependency, suggesting that the epitopes of these mAbs differ. Interestingly, the mAbs were least able to neutralize Anhui-RG5. This may reflect the genetic distance between Anhui-RG5 (clade 2.3) and NIBRG-14 (clade 1).

Antigen-capture ELISA: To quantitatively detect H5N1 virus, we constructed a sandwich ELISA-based virus antigen-capture detection system. Preliminary experiments tested all combinations of two mAbs from the eight mAbs; Niid_H5F had the highest detection sensitivity for purified H5N1 virion and reacted broadly to the H5_HA of viruses belonging to clades 1, 2.1, 2.2, and 2.3. Therefore, Niid_H5F was selected as the antigen-capturing mAb. The antigen-capture ELISA was constructed by immobilizing Niid_H5F (and/or Niid_H5C) on the ELISA plate and using biotinylated Niid_H5D as the detection mAb, since this combination gave the best results (data not shown). Since the eight mAbs

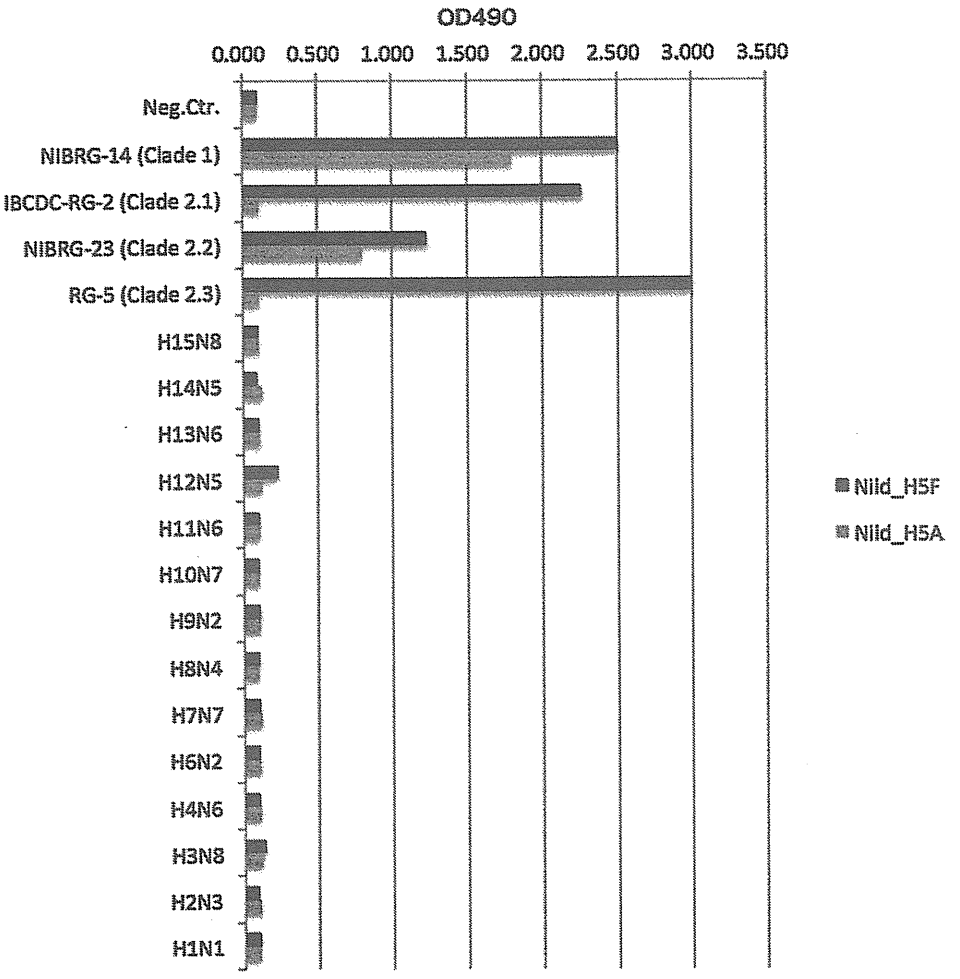

Fig. 4. ELISA reactivity of the Niid_H5A and Niid_H5F monoclonal antibodies (mAbs) to various influenza virus strains. Different influenza virus strains were immobilized on 96-well plates and incubated with biotinylated Niid_H5A or Niid_H5F mAbs followed by peroxidase-labeled streptavidin. The binding of the mAbs was then quantitated by a colorimetric assay using TMB as a substrate.

were originally raised against the H5N1 virus strain A/Vietnam/1194/2004 (NIBRG-14), the validity of this system with other strains of H5N1 virus was also examined. As shown in Fig. 4, this system could detect the A/Indonesia/05/2005 (Indo5/PR-8-RG2), A/Turkey/1/2005 (NIBRG-23), and A/Anhui/01/2005 (Anhui01/PR8-RG5) strains but none of the non-H5N1 strains. The sandwich ELISA could detect H5N1 virus protein at concentrations as low as 50 ng/mL HA, namely, >3 SD of negative samples (Fig. 5).

DISCUSSION

In the present study, mAbs against H5N1 influenza virus were established. These mAbs could detect the virus when used in Western blot analyses, IFA, immunohistochemical analyses, neutralization assays, and antigen-capture ELISA. The characteristics of the mAbs are summarized in Table 1.

Of the eight mAb clones that reacted to H5N1 virus in ELISAs, six reacted to rHA. Only one clone reacted to NA protein. Another clone detected an unknown 150-kDa molecule upon Western blot analysis. A hybridoma that secreted a mAb that could detecte the nuclear protein or other protein components of H5N1 virus was not detected, presumably because the first screening step identified H5 specificity. These results indicate that the HA protein is a dominant target in the antibody response of HA-subtype specificity, as suggested by other studies (17,18). There is accumulating evidence that the influenza strain-specific epitopes are often localized on the HA1 region, whereas the epitopes that are conserved among various strains are localized on the HA2 region (19–22). It has been reported that the immune response elicited by H1N1pdm yields a high frequency of HA2-specific mAbs (23,24). In the present study, none of the established clones detected the HA2 fragment of H5HA, presumably because this study focused on H5-specific clones.

The mAbs isolated in the present study were assessed for their ability to detect H5N1 virus-infected MDCK cells in IFA. Indeed, the anti-HA and anti-NA mAbs detected the cytoplasmic Golgi-rich region and the cell surface membrane. This reflects the common assembly process of influenza virus (25).

In general, a single diagnostic test is not reliable because of the potential for false positives and negatives. Considering the restricted availability of RNA detection systems (26,27), serological screening systems other than those that detect antibodies are currently being ex-

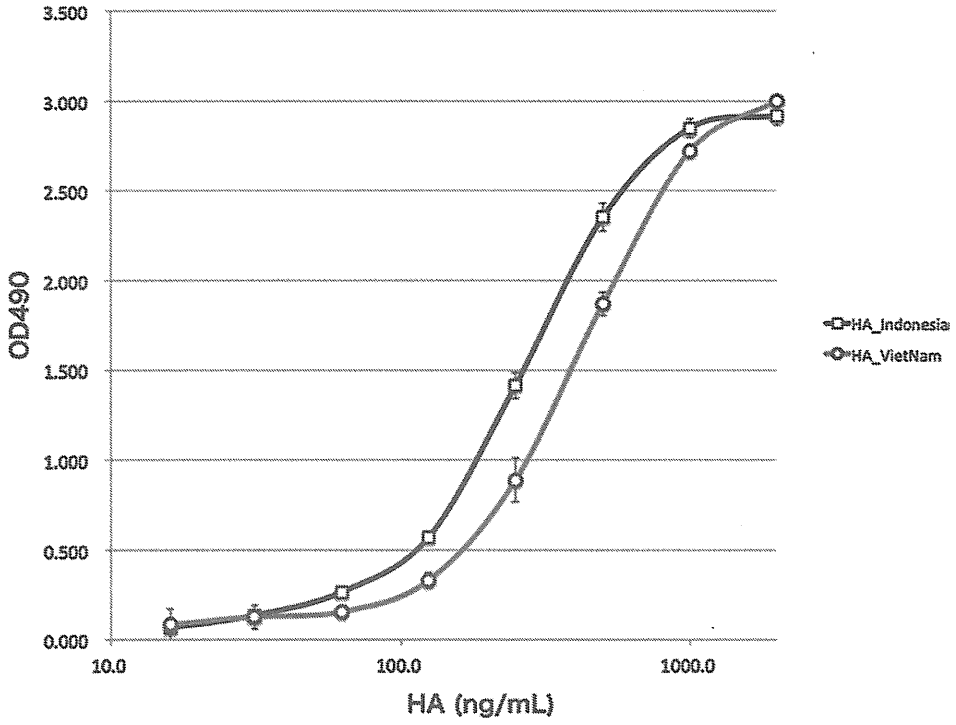

Fig. 5. Antigen-capture ELISA reactivity of monoclonal antibodies (mAbs) to H5N1 and H1N1 virus strains. The anti-H5 mAb Niid_H5F was immobilized on 96-well plates and reacted with serially-titrated purified H5N1 virus fractions for 1 h at room temperature. The bound virus proteins were detected by incubation with biotinylated Niid_H5D (anti-H5) antibody followed by peroxidase-labeled streptavidin. The binding was quantitated by a colorimetric assay that used TMB as a substrate. Abscissa, concentration of purified H5N1 virus proteins. Ordinate, absorbance unit (OD490).

amined. ELISA-based antigen-capture assays offer high specificity and reproducibility and have been used to diagnose and monitor many diseases. The present study describes the development of an antigen-capture ELISA system that detects purified H5N1 virus virion at levels as low as 50 ng/mL. The sensitivity of this system, which comprises three anti-HA mAbs, appears sufficiently high to detect virus protein in patient sera, particularly since a recently reported antigen-capture ELISA system detects 50 ng/mL of purified recombinant HA1 protein (28). At present, the sensitivity of the system is being improved, and its usefulness in diagnosing and monitoring H5N1 virus infections is being validated.

The five selected anti-HA mAbs exhibited significant neutralization activity against several viral strains in a clade-dependent manner (Table 2). Of these, Niid_H5F showed the broadest spectrum of neutralization activity, but it neutralized NIBRG-23 (clade 2.2) more efficiently than the original immunogen NIBRG-14 (clade 1). It would be of interest to determine the features that determine this clade-dependency of mAb recognition. It is also possible that these mAbs have therapeutic potential, if humanized by means of complementarity determining region grafting or mouse-human chimerism.

In conclusion, eight new H5N1-specific mAbs were generated from A/Vietnam/1194/2004 (NIBRG-14)-hyperimmunized mice, six of which were HA-specific. These mAbs were useful in Western blot analyses, IFA, and immunohistology and had in vitro neutralization activity against H5N1 viruses. These mAbs also perform well in a highly sensitive antigen-capture sandwich ELISA system. As such, these mAbs may be useful for the rapid and specific diagnosis of H5N1 subtype influenza virus and may have therapeutic potential.

Acknowledgments We are grateful to Ms. Sayuri Yamaguchi, Yuko Sato, and Yukari Hara for their assistance in establishing the hybridomas. We also thank Dr. Le Mai Thi Quynh at the National Institute of Hygiene and Epidemiology, Vietnam for supplying the A/Vietnam/1194/2004 virus and Dr. John Wood at NIBSC for providing the NIBRG-14 virus.

This work was supported by grants from the Ministry of Health, Labour and Welfare of Japan and from Health Science Foundation of Japan.

Conflict of interest None to declare.

REFERENCES

1. Chan, M.C., Cheung, C.Y., Chui, W.H., et al. (2005): Proinflammatory cytokine responses induced by influenza A (H5N1) viruses in primary human alveolar and bronchial epithelial cells. Respir. Res., 6, 135.
2. World Health Organization Global Influenza Program Surveillance Network (2005): Evolution of H5N1 avian influenza viruses in Asia. Emerg. Infect. Dis., 11, 1515-1521.
3. Webster, R.G. and Govorkova, E.A. (2006): H5N1 influenza—continuing evolution and spread. N. Engl. J. Med., 355, 2174-2177.
4. Webster, R.G., Guan, Y., Peiris, M., et al. (2002): Characterization of H5N1 influenza viruses that continue to circulate in geese in southeastern china. J. Virol., 76, 118-126.
5. World Health Organization: Online at 〈http://www.who.int/csr/disease/avian_influenza/country/cases_table_2011_2008_2019/en/index.html〉.
6. Uyeki, T.M. (2009): Human infection with highly pathogenic avian influenza A (H5N1) virus: review of clinical issues. Clin. Infect. Dis., 49, 279-290.